

# The Higgs condensate as a quantum liquid: A critical comparison with observations

Paolo Cea <sup>1</sup>

*INFN - Sezione di Bari, Via Amendola 173 - 70126 Bari, Italy*

## Abstract

The triviality of four-dimensional scalar quantum field theories poses challenging problems to the usually adopted perturbative implementation of the Higgs mechanism. In the first part of the paper we compare the triviality scenario and the renormalised two-loop perturbation theory to precise and extensive results from non-perturbative numerical simulations of the real scalar field theory on the lattice. The proposal of triviality and spontaneous symmetry breaking turns out to be in good agreement with numerical simulations, while the renormalised perturbative approach seems to suffer significant deviations from the numerical simulation results. In the second part of the paper we try to illustrate how the triviality of four-dimensional scalar field theory leads, nevertheless, to the spontaneous symmetry breaking in the scalar sector of the Standard Model. We show how triviality allows us to develop a physical picture of the Higgs mechanism in the Standard Model. We suggest that the Higgs condensate behave like a relativistic quantum liquid leading to the prevision of two Higgs bosons. The light Higgs boson resembles closely the new LHC narrow resonance at 125 GeV. The heavy Higgs boson is a rather broad resonance with mass of about 730 GeV. We critically compare our proposal to the complete LHC Run 2 data collected by the ATLAS and CMS Collaborations. We do not find convincingly evidences of the heavy Higgs boson in the ATLAS datasets. On the other hand, the CMS full Run 2 data display evidences of a heavy Higgs boson in the main decay modes  $H \rightarrow WW$ , while in the preliminary Run 2 data there are hints of the decays  $H \rightarrow ZZ$  in the golden channel. We also critically discuss plausible reasons for the discrepancies between the two LHC experiments.

Keywords: Lattice Field Theory; Higgs Boson; Higgs production mechanisms; Higgs decays

PACS: 11.10.-z; 11.15.Ex; 14.80.Bn; 12.15.-y

---

<sup>1</sup>Electronic address: [paolo.cea@ba.infn.it](mailto:paolo.cea@ba.infn.it)

# Contents

<b>1</b>	<b>Introduction</b>	<b>3</b>
<b>2</b>	<b>Triviality and spontaneous symmetry breaking</b>	<b>5</b>
<b>3</b>	<b>Comparison with non-perturbative numerical simulations</b>	<b>11</b>
<b>4</b>	<b>The quantum liquid picture</b>	<b>22</b>
<b>5</b>	<b>Comparison with experimental observations</b>	<b>26</b>
5.1	Comparison with the ATLAS Run 2 datasets . . . . .	29
5.2	Comparison with the CMS Run 2 datasets . . . . .	32
<b>6</b>	<b>Summary and conclusions</b>	<b>38</b>

# 1 Introduction

Scalar quantum field theories in four dimensions are of fundamental interest since they play a fundamental role in the Standard Model giving rise to the generation of fermion and gauge boson masses via the Higgs mechanism [1, 2, 3, 4]. In 2012 a new particle was discovered by the ATLAS and CMS experiments at the Large Hadron Collider (LHC) [5, 6]. This new particle, with a mass of about 125 GeV, turned out to be consistent with the Standard Model Higgs boson thereby validating the Higgs mechanism.

In the Standard Model of Particle Physics the Higgs mechanism is implemented by introducing scalar fields, the Higgs fields, with a specific potential. In the generally accepted picture, the spontaneous symmetry breaking in the Standard Model is managed within the perturbation theory which leads to the prediction that the Higgs boson mass squared is proportional to  $\lambda v^2$ , where  $\lambda$  is the positive scalar self-coupling and  $v \simeq 246$  GeV is the known weak scale. To do this, first one assume that the quantum Higgs fields undergo the condensation by means of a tachyonic mass term  $\mu^2 < 0$ . After that, it is assumed the existence of a short-range repulsion, assured by the positive quartic self-coupling, to stabilise the condensation of the Higgs fields. This description of a fundamental aspect of the Standard Model is highly unsatisfactory. The first problem comes out from the tachyonic mass term. Indeed, there are no physical mechanisms able to generate a negative squared mass. So that assuming the presence of the tachyonic mass is simply unjustified. In other words, one is assuming that for some reasons the Higgs fields are condensing in the ground state. The second problem arises from the fact that self-interacting scalar fields in four space-time dimensions are subject to the triviality problem [7], namely the renormalised self-coupling  $\lambda \rightarrow 0$  when the ultraviolet cutoff is sent to infinity. Strictly speaking, up to now there was no rigorous proof of triviality. However, extensive non-perturbative numerical studies in four dimensions had convincingly confirmed the triviality conjecture. On the other hand, it is worthwhile to mention that in the recent paper Ref. [8] it has been rigorously demonstrated the triviality of the scaling limits of the Ising and self-interacting scalar field models in four dimensions. Namely, the scaling limits of the critical Ising and self-interacting scalar field in four dimensions are Gaussian as Euclidean field theories. Thus, we see that there are no more doubts on the Gaussian, or triviality, nature of one-component self-interacting scalar quantum field theory.

Actually, in the usual implementation of the renormalised perturbation theory it is assumed that trivial scalar field theories exist and may be far from being free provided one allows for a large but finite ultraviolet cutoff  $\Lambda$ . For instance, the cutoff  $\Lambda$  may be introduced explicitly by a lattice with finite lattice spacing  $a$ . In any case, in Minkowski space-time one must admit that the momenta are constrained by:

$$|k_\mu| \lesssim \Lambda \quad , \quad \mu = 0, 1, 2, 3 \quad , \quad (1.1)$$

while, equivalently, in the Euclidean field theory on a hypercubic lattice:

$$|k_i| \lesssim \Lambda \simeq \frac{\pi}{a} \quad , \quad i = 1, 2, 3, 4 \quad . \quad (1.2)$$

The innocently looking condition Eq. (1.1), or the Euclidean version Eq. (1.2), is routinely employed in perturbative calculations by means of Feynman diagrams. However, quantum field theories are not a mere collection of Feynman diagrams. The general theory of relativistic quantised fields is formulated in terms of fields  $\hat{\phi}(x)$  that are operator-valued

tempered distributions densely defined in the Hilbert space of physical states (see, for instance, Refs. [9, 10]). The singular behaviour of the fields as a function of the spacetime point  $x$  is an inevitable consequence of relativistic covariance. In fact, there is a pertinent theorem due to Wightman [11] that says that, if one assumes that a quantum field exists as an (in general unbounded) operator at a spacetime point  $x$  and it is covariant with respect to a (strongly continuous) unitary representation of the Poincare group, then the quantum field is trivial in the sense that it is a multiple of the identity. In other words, the Hilbert space of the physical states should consist only of the vacuum state. It is worthwhile to stress that the theorem holds only if the quantum field is local. Thus, we may evade the Wightman theorem if the quantum field is non-elementary or compound. By the Wightman theorem we know that the local quantum field must be singular. More precisely, we already said that the quantum field operator  $\hat{\phi}(x)$  must be a (tempered) distribution whose singularities are at most finite derivatives of the Dirac  $\delta$  distribution. If we admit the validity of Eq. (1.1), or Eq. (1.2), then the Dirac  $\delta$  distribution becomes a non-singular fat  $\delta$ -function and, therefore, the quantum scalar field is a non-singular operator so that the Hilbert space of the physical states becomes empty. This shows that we cannot evade the triviality problem for relativistic local scalar quantum fields. The unique way out left would be to consider the Higgs scalar fields as non-elementary. In this case the cutoff  $\Lambda$  must be interpreted as a high-energy scale such that, for distances smaller than  $1/\Lambda$ , the Higgs fields are replaced by unknown elementary quantum fields. However, the problem is that, up to now, the experimental observations at the Large Hadron Collider did not display any signs of physics beyond the Standard Model. So that we are led to exclude these mundane possibilities.

There is another problematic aspect that affects the perturbative treatment of the Higgs mechanism. As a matter of fact, the naive perturbation theory overlooks the fact that, according to the Haag's theorem [12]<sup>2</sup>, the quantum vacuum with scalar condensate is inequivalent to the perturbative quantum vacuum, i.e. the free massive scalar field quantum vacuum. Here inequivalent means that the two vacua are not connected by a unitary transformation. In particular, as we shall discuss later on, the presence of the scalar condensate imposes a constraint on the scalar quantum field that, according to a seminal paper by K. Symanzik [17] on the Schrödinger representation and Casimir effect in quantum field theories, requires a renormalisation of the condensate strength that is different from the usual wavefunction renormalisation constant. This should completely jeopardise the perturbative approach such that the renormalised perturbative calculations could lead to misleading results.

The aim of the present paper is twofold. Firstly, in Sect. 2 we argue that spontaneous symmetry breaking in a relativistic local quantum scalar field theory is not incompatible with the triviality of the theory. To this end, we focus on a real massless scalar field and show that quantum fluctuations can drive the scalar condensation if one admits an even infinitesimal positive quartic self-coupling. The essence of the mechanism practically coincides with the one-loop evaluation of the effective potential performed in the classical paper by Coleman and Weinberg [18] (see, also, Ref. [19]). Note that the suggestion of the coexistence of spontaneous symmetry breaking with triviality has been already advanced since long time in Ref. [20, 21]. In Sect. 3 we compare the triviality and symmetry breaking scenario as well as the renormalised two-loop perturbation theory approach to precise

---

<sup>2</sup>The interested readers can find a rather complete account on the Haag's theorem in Refs. [13, 14, 15, 16]

and extensive results from non-perturbative numerical simulations of the real scalar field theory on the lattice. Here we shall see that the triviality and spontaneous symmetry breaking proposal is in quite good agreements with the available results from numerical simulations, while the renormalised perturbative approach displays significant deviations from the numerical simulation outcomes.

In the second part of the paper, we apply the triviality and spontaneous symmetry breaking mechanism to the scalar sector of the Standard Model. We develop a physical picture of the Higgs mechanism in the Standard Model which is not subject to the naturalness and stability problems. In Sect. 4 we further illustrate the suggestion, already advanced in a previous paper [22], that the Higgs condensate behaves as the relativistic version of a quantum liquid much like the He II in the superfluid phase. This proposal lead to the remarkable result that the Higgs condensate excitations behave as two Higgs bosons. The light Higgs boson was already identified with the new LHC narrow resonance at 125 GeV [22]. On the other hand, the heavy Higgs boson turns out to a broad resonance with central mass of about 730 GeV. In Sect. 5 we critically contrast our theoretical proposal to the complete Run 2 datasets from both ATLAS and CMS experiments. In particular, we looked at evidences for our heavy Higgs boson. We anticipate that we did not find convincingly evidences of the heavy Higgs boson in the ATLAS data (Sect. 5.1). On the contrary, the CMS data (Sect. 5.2) seem to display reasonable evidences of a heavy Higgs boson in the main decay channels  $H \rightarrow VV$ ,  $V=W, Z$  that compare quite favourably to our theoretical proposal. Finally, in Sect. 6 we briefly summarise the main results of the paper and draw our conclusions.

## 2 Triviality and spontaneous symmetry breaking

In this section we would like to illustrate the triviality and spontaneous symmetry breaking scenario within the simplest scalar quantum field theory, namely the one-component quantum scalar field  $\hat{\phi}(x)$ . To start with, we recall the spontaneous symmetry breaking mechanism in the standard treatment. Let us consider the Lagrangian:

$$\mathcal{L} = \frac{1}{2} (\partial_\mu \hat{\phi})^2 - \frac{1}{2} \mu^2 \hat{\phi}^2 - \frac{1}{4} \lambda_0 \hat{\phi}^4, \quad (2.1)$$

where  $\lambda_0$  and  $\hat{\phi}$  are the bare quartic self-coupling and quantum field respectively. The mass parameter  $\mu^2$  is assumed to be negative (tachyonic mass term) so that the quantum scalar field is forced to develop a non-zero vacuum expectation value  $\phi$ . Due to the translational invariance of the quantum vacuum  $\phi$  must be a real number, i.e. the scalar condensate is time-independent and spatially uniform. After that the true quantum vacuum is obtained by writing  $\phi = v$ , where  $v$  is obtained by minimising the classical potential term in the Lagrangian Eq. (2.1), and

$$\hat{\phi}(x) = \hat{\eta}(x) + v. \quad (2.2)$$

One readily obtains that the shifted quantum field  $\hat{\eta}(x)$  is a massive scalar field with mass  $m^2 = 2\lambda_0 v^2$  and with quartic and cubic self-interaction terms. However, as we said in the Introduction, this approach is highly questionable since there are no physical mechanisms able to generate a negative squared mass for a local quantum scalar field. We are led, therefore, to assume  $\mu^2 = 0$ . In this case the minimum of the classical potential is at  $v = 0$ . The only way out left is to hope that quantum fluctuations could

induce the vacuum condensation of the scalar field. To check this we need to evaluate the effective potential that includes the quantum corrections to the classical potential. The effective potential can be systematically evaluated in an expansion in power of the Planck's constant. The lowest order approximation corresponds to the one-loop approximation. As it is well known [18], the lowest order effective potential is obtained by summing the one-loop vacuum diagrams:

$$V_{1-loop}(\phi) = \frac{1}{4}\lambda_0 \phi^4 - \frac{i}{2} \int \frac{d^4 k}{(2\pi)^4} \ln[-k_0^2 + \vec{k}^2 + 3\lambda_0 \phi^2 - i\epsilon]. \quad (2.3)$$

Integrating over  $k_0$  and discarding an inessential constant gives:

$$V_{1-loop}(\phi) = \frac{1}{4}\lambda_0 \phi^4 + \frac{1}{2} \int \frac{d^3 k}{(2\pi)^3} \sqrt{\vec{k}^2 + 3\lambda_0 \phi^2}. \quad (2.4)$$

This last equation offers an interesting interpretation of the one-loop effective potential. In fact, Eq. (2.4) shows that the  $V_{1-loop}(\phi)$  can be interpreted as the free vacuum energy density of the shifted field  $\hat{\eta}(x)$ . To see this we note that in the quadratic approximation the Hamiltonian of the fluctuation over the condensate background  $\hat{\eta}$  is given by:

$$\hat{\mathcal{H}}_0 = \frac{1}{2}\hat{\Pi}_\eta^2(x) + \frac{1}{2}(\vec{\nabla}\hat{\eta}(x))^2 + \frac{1}{2}(3\lambda_0 \phi^2)\hat{\eta}^2(x) + \frac{1}{4}\lambda_0 \phi^4, \quad (2.5)$$

where  $\hat{\Pi}_\eta(x)$  is the conjugate momentum of the fluctuating field.

Performing the integrals in Eq. (2.4) and introducing an ultraviolet cutoff  $\Lambda$ , after mass renormalisation [18, 19], one obtains easily:

$$V_{1-loop}(\phi) = \frac{1}{4}\lambda_0 \phi^4 + \frac{\omega(\phi)^4}{64\pi^2} \ln\left(\frac{\omega^2(\phi)}{\Lambda^2}\right), \quad \omega^2(\phi) = 3\lambda_0 \phi^2. \quad (2.6)$$

A straightforward calculation shows that the one-loop effective potential displays a minimum at:

$$3\lambda_0 v^2 = \frac{\Lambda^2}{\sqrt{e}} \exp\left[-\frac{16\pi^2}{9\lambda_0}\right]. \quad (2.7)$$

Indeed, one can easily check that:

$$V_{1-loop}(v) = -\frac{\omega^4(v)}{128\pi^2}, \quad (2.8)$$

Using Eq. (2.7) we can rewrite Eq. (2.6) as:

$$V_{1-loop}(\phi) = \frac{\omega^4(\phi)}{64\pi^2} \left[ \ln\left(\frac{\phi^2}{v^2}\right) - \frac{1}{2} \right]. \quad (2.9)$$

Since we are dealing with a renormalisable theory, the effective potential must satisfy the renormalisation group invariance. So that for  $\Lambda \rightarrow \infty$  we have:

$$\left[ \Lambda \frac{\partial}{\partial \Lambda} + \beta \frac{\partial}{\partial \lambda_0} + \gamma \phi \frac{\partial}{\partial \phi} \right] V_{1-loop}(\phi) = 0, \quad (2.10)$$

where  $\gamma$  is the anomalous dimension of the quantum scalar field related to the wavefunction renormalisation constant and the beta-function is defined by:

$$\Lambda \frac{\partial}{\partial \Lambda} \lambda = \beta(\lambda) . \quad (2.11)$$

In the previous equations we are considering the bare coupling constant as the quartic self-coupling at the cutoff scale  $\Lambda$ . The renormalisation process tells us that we can change the bare coupling  $\lambda_0$  and the ultraviolet cutoff  $\Lambda$  while, at the same time, keeping the renormalised coupling constant fixed at some value. Within perturbation theory one finds [18, 19]:

$$\gamma_{pert} = 0 \quad , \quad \beta_{pert}(\lambda) = \frac{9}{8\pi^2} \lambda^2 . \quad (2.12)$$

Thus, the one-loop corrections have generated spontaneous symmetry breaking. However, the minimum of the effective potential lies outside the expected range of validity of the one-loop approximation and it must be rejected as an artefact of the approximation. Indeed, the renormalisation group resummed effective potential does not display symmetry breaking. On the other hand, as discussed in Section 1, there are no doubt on the triviality of the theory. As a consequence, within perturbation theory there is no room for symmetry breaking in a self-interacting scalar field theory. However, following the suggestion of Refs. [20, 21] we argue below that spontaneous symmetry breaking could be compatible with the triviality of the scalar quantum field theory. The arguments go as follows. Let us suppose that, notwithstanding the triviality problem, the massless quantum scalar field  $\hat{\phi}(x)$  undergoes the vacuum condensation. This means that, according to Eq. (2.2), the quantum field can be decomposed into the fluctuating quantum field  $\hat{\eta}(x)$  and the uniform vacuum condensate  $\phi$ . In this case the triviality of the theory means that the quantum fluctuation must be a free field. The presence of the vacuum scalar condensate suggests that  $\hat{\eta}(x)$  is a massive free field. Our previous one-loop perturbative discussion indicated that the vacuum condensation and scalar mass generation of the fluctuating field could originate from vacuum quantum fluctuations. Now, the quantum fluctuations of free field are Gaussian and, thereby, cannot induce dynamically the spontaneous symmetry breaking we are looking for. Our previous discussion of the Coleman and Weinberg mechanism showed that the dynamical spontaneous symmetry breaking requires the presence of non-Gaussian vacuum fluctuations introduced by a positive quartic self-coupling  $\lambda_0 > 0$ . The presence of the quartic self-coupling leads to the vacuum condensation of the scalar field and gives rise to a mass term for the free fluctuating quantum field without introducing any new interaction terms to be consistent with the triviality nature of the quantum scalar field. Obviously, the requirement of a finite quartic self-coupling is in striking contradiction with the triviality of the theory. For the time being, we simply adopt we above assumptions. It should be clear that, to be consistent, we must send the quartic self-coupling to zero at the end of our calculations. We will return on this delicate point later on.

From the above discussion it follows that the quantum Hamiltonian of the quantum field  $\hat{\eta}(x)$  is the free Hamiltonian operator:

$$\hat{\mathcal{H}} = \frac{1}{2} \hat{\Pi}_\eta^2(x) + \frac{1}{2} (\vec{\nabla} \hat{\eta}(x))^2 + \frac{1}{2} \tilde{\omega}^2(\phi) \hat{\eta}^2(x) + \frac{1}{4} \lambda_0 \phi^4 , \quad (2.13)$$

where:

$$\tilde{\omega}^2(\phi) = 3 \tilde{\lambda} \phi^2 , \quad \tilde{\lambda} = a_1 \lambda_0 , \quad (2.14)$$

where  $a_1$  is some numerical constant. Note that for  $a_1 = 1$  we recover the one-loop effective Hamiltonian Eq. (2.5), while  $a_1 = 2/3$  corresponds to the variational Gaussian approximation. The actual value of the parameter  $a_1$  will be fixed in the next Section by comparing with non-perturbative numerical simulations of the Euclidean version of the quantum scalar theory. Since the quantum Hamiltonian is quadratic in the fields, the *exact* effective potential is simply the vacuum energy density:

$$V_{triv}(\phi) = \frac{1}{4}\lambda_0\phi^4 + \frac{1}{2}\int\frac{d^3k}{(2\pi)^3}\sqrt{\vec{k}^2 + \tilde{\omega}^2(\phi)} = \frac{1}{4}\lambda_0\phi^4 + \frac{\tilde{\omega}^4(\phi)}{64\pi^2}\ln\left(\frac{\tilde{\omega}^2(\phi)}{\Lambda^2}\right). \quad (2.15)$$

As in the previous one-loop calculations the triviality effective potential displays a minimum at:

$$3\tilde{\lambda}v^2 = \frac{\Lambda^2}{\sqrt{e}}\exp\left[-\frac{16\pi^2}{9\tilde{\lambda}}\right]. \quad (2.16)$$

Introducing:

$$m_H^2 = \tilde{\omega}^2(v) = 3\tilde{\lambda}v^2, \quad (2.17)$$

we recast the effective potential into the form:

$$V_{eff}(\phi) = \frac{(3\tilde{\lambda}\phi^2)^2}{64\pi^2}\left[\ln\left(\frac{3\tilde{\lambda}\phi^2}{m_H^2}\right) - \frac{1}{2}\right]. \quad (2.18)$$

This last equation shows that:

$$V_{triv}(v) = -\frac{m_H^4}{128\pi^2}, \quad (2.19)$$

confirming that the effective potential has a negative minimum at  $\phi = v$ . Now the problem is to see if it exists the continuum limit  $\Lambda \rightarrow \infty$  and if this limit is consistent with the triviality of the theory. Obviously, we must have:

$$\left[\Lambda\frac{\partial}{\partial\Lambda} + \beta(\lambda_0)\frac{\partial}{\partial\lambda_0} + \gamma(\lambda_0)\phi\frac{\partial}{\partial\phi}\right]V_{triv}(\phi) = 0. \quad (2.20)$$

Note that, at variance of the perturbative approach, we cannot use perturbation theory to determine  $\beta(\lambda_0)$  and  $\gamma(\lambda_0)$ . First, we may use Eq. (2.20) at the minimum  $v$  where the derivative of the effective potential vanishes. We get:

$$\left[\Lambda\frac{\partial}{\partial\Lambda} + \beta(\lambda_0)\frac{\partial}{\partial\lambda_0}\right]m_H^2 = 0. \quad (2.21)$$

This last equation shows that  $m_H^2$  is a renormalisation-group invariant physical quantity. Thus, the renormalisation procedure has introduced an arbitrary dimensional parameter (dimensional transmutation).

Let us, now, solve Eq. (2.21). We get:

$$\beta_{triv}(\lambda_0) = -a_1\frac{9}{8\pi^2}\lambda_0^2. \quad (2.22)$$

After that, inserting Eq. (2.22) into Eq. (2.20) we finally obtain:

$$\gamma_{triv}(\lambda_0) = -a_1\frac{9}{16\pi^2}\lambda_0. \quad (2.23)$$



From Eqs. (2.22) and (2.23) we see that:

$$\frac{\gamma_{triv}(\lambda)}{\beta_{triv}(\lambda)} = -\frac{1}{2\lambda} . \quad (2.24)$$

A few comments are in order. Firstly, Eq. (2.22) shows that the beta-function is negative. As a consequence, the theory is free asymptotically in agreement with triviality:

$$\lim_{\Lambda \rightarrow \infty} \lambda \sim \frac{16\pi^2}{9a_1} \frac{1}{\ln\left(\frac{\Lambda^2}{m_H^2}\right)} . \quad (2.25)$$

It is worthwhile to note that the asymptotic behaviour of the self-coupling constant  $\lambda$  does not depend on the bare parameter  $\lambda_0$ . The triviality of the theory means that the fluctuating quantum field  $\hat{\eta}(x)$  is a free field. On the other hand, a non-zero value of the anomalous dimension  $\gamma_{triv}$  indicates that the scalar condensate suffers a non-trivial renormalisation. Let us introduce the renormalised field  $\hat{\eta}_R(x)$  and condensate  $\phi_R$ . Since the fluctuation  $\hat{\eta}$  is a free field with mass  $m_H$  we have  $\hat{\eta}_R = \hat{\eta}$ , namely:

$$Z_\eta = 1 . \quad (2.26)$$

On the other hand, for the scalar condensate we have:

$$\phi_R = Z_\phi^{-\frac{1}{2}} \phi , \quad (2.27)$$

where, according to Eq. (2.23), we have:

$$\lim_{\Lambda \rightarrow \infty} Z_\phi \sim \frac{9a_1}{16\pi^2} \ln\left(\frac{\Lambda^2}{m_H^2}\right) . \quad (2.28)$$

Finally, Eq. (2.24) assures that both  $m_H^2 = 3\tilde{\lambda}v^2$  and  $\tilde{\omega}^2(\phi) = 3\tilde{\lambda}\phi^2$  are renormalisation group invariants. This, in turns, shows that  $V_{triv}(\phi)$ , as given by Eq. (2.18), is manifestly renormalisation group invariant. To see this, we note that:

$$\ln \sqrt{\frac{Z_\phi(\mu)}{Z_\phi(\mu_0)}} = \int_{\lambda(\mu_0)}^{\lambda(\mu)} \frac{\gamma_{triv}(\lambda')}{\beta_{triv}(\lambda')} d\lambda' = -\frac{1}{2} \int_{\lambda(\mu_0)}^{\lambda(\mu)} \frac{d\lambda'}{\lambda'} = -\frac{1}{2} \ln \frac{\lambda(\mu)}{\lambda(\mu_0)} . \quad (2.29)$$

Therefore we have:

$$Z_\phi(\mu) \lambda(\mu) = Z_\phi(\mu_0) \lambda(\mu_0) . \quad (2.30)$$

Another remarkable consequence of Eq. (2.30) is that, after using Eqs. (2.25) and (2.28), the physical mass  $m_H$  is *finitely* related to the renormalised vacuum expectation value of the scalar field  $v_R$ :

$$m_H = \xi v_R . \quad (2.31)$$

It should be clear that the physical mass  $m_H$  is an arbitrary parameter of the theory. On the other hand the parameter  $\xi$  being a pure number can be determined in the non perturbative lattice approach.

The above discussion indicates that the triviality and spontaneous symmetry breaking approach deviates considerably from the perturbative scheme. In particular, in the triviality proposal the scalar condensate is subject to a non-trivial rescaling  $Z_\phi$  which is

different from the wavefunction renormalisation constant  $Z_\eta$  of the fluctuating field. We suspect that it is this aspect that led to a widespread skepticism toward the triviality and spontaneous symmetry breaking proposal. The crucial point is that the perturbative approach completely neglects the quantum-mechanical nature of the vacuum condensation of the scalar field. In fact, we show below that the scalar condensation is the relativistic version of the Bose-Einstein condensation that, as it is well known, is a purely quantum phenomenon. As we said, in the perturbative implementation of the vacuum condensation of the quantum scalar field one introduces a tachyonic mass term that drives the condensation in the vacuum. This process is stabilised by the presence of a repulsive quartic self-coupling. As a result the vacuum scalar condensate strength  $v$  is evaluated by minimising the classical potential. After that, the higher order corrections are evaluated by means of the perturbative expansion in the small self-coupling. We see, therefore, that it is implicitly believed that the vacuum scalar condensation is essentially a semi-classical process. This is not true. Indeed, let us consider the vacuum expectation value of the quantum scalar field  $\hat{\phi}(x)$ . Since the Hamiltonian operator annihilates the vacuum, without loss in generality, we may assume  $t = 0$ . Then:

$$v = \langle \hat{\phi}(\vec{x}) \rangle = \frac{1}{V} \left\langle \int d\vec{x} \hat{\phi}(\vec{x}) \right\rangle , \quad (2.32)$$

where  $V$  is the spatial volume and we have used the translational invariance of the vacuum. In terms of the Fourier transform of the quantum field:

$$\hat{\phi}(\vec{k}) = \int \frac{d\vec{x}}{(2\pi)^{3/2}} \exp(i\vec{k} \cdot \vec{x}) \hat{\phi}(\vec{x}) , \quad (2.33)$$

Eq. (2.32) reads:

$$\langle \hat{\phi}(\vec{k} = 0) \rangle = \frac{V}{(2\pi)^{3/2}} v . \quad (2.34)$$

Therefore, we see that the zero modes of the quantum field  $\hat{\phi}(\vec{k})$  are macroscopically occupied. In other words the quantum field  $\hat{\phi}$  suffered the Bose-Einstein condensation. Moreover, since the zero-modes  $\hat{\phi}(\vec{k} = 0)$  become macroscopically occupied, the creation and annihilation operators  $\hat{a}_{\vec{k}=0}^\dagger$  and  $\hat{a}_{\vec{k}=0}$  are no longer operators but they can be considered c-numbers. This corresponds exactly to the approximations adopted by N. N. Bogolubov in his attempt to explain the phenomenon of superfluidity in He II from first principles [23]. We, therefore, may conclude that the physical meaning of Eq. (2.2) is the Bose-Einstein condensation of the relativistic local quantum field  $\hat{\phi}$  in the Bogolubov's approximations. It follows that the Bose-Einstein condensation leads to the following constraints on the quantum field  $\hat{\phi}(\vec{k})$ :

$$\hat{\phi}(\vec{k}) \Big|_{\vec{k}=0} = \frac{V}{(2\pi)^{3/2}} v . \quad (2.35)$$

We are led to a scalar quantum field with Dirichlet boundary conditions on the hypersurface  $\vec{k} = 0$ . In a classical paper by K. Symanzik on the Schrödinger representation in quantum field theories [17] it was demonstrated that the field operator that is being diagonalised on a smooth hypersurface differs from the usual renormalised field by a diverging factor. In our case the divergency related to the presence of the boundary condition can be eliminated by adding one more counterterm to the usual counterterms. More precisely,

we need to renormalise the zero-mode quantum field  $\hat{\phi}(\vec{k})|_{\vec{k}=0}$  with a renormalisation constant ( $Z_\phi$ ) that is different from the usual wavefunction renormalisation constant ( $Z_\eta$ ) of the fluctuating fields  $\hat{\phi}(\vec{k}), \vec{k} \neq 0$ . Another important aspect to be considered is that the creation and annihilation operators of the vacuum with condensate are related to the ones of the vacuum without condensate by the Bogolubov's canonical transformations [23]. As a consequence, the two vacua are inequivalent in accordance with the Haag's theorem. The usually adopted perturbative scheme, by considering the vacuum scalar condensation as a quasi-classical phenomenon, completely overlooks these important aspects. Therefore, we see that the renormalised perturbative approach could lead to misleading results. Let us summarise the main results of this rather technical Section. Basically, what we have shown is that a free massless scalar quantum field in presence of an even infinitesimal positive quartic self-coupling is unstable towards the phase with Bose-Einstein condensation. As a result, the stable phase is a massive free scalar field and a finite scalar vacuum condensate where the scalar field mass is finitely related to the vacuum condensate strength.

The problem is that, within the pure scalar sector, we do not have a physical mechanism to generate a positive self-coupling needed to trigger the spontaneous symmetry breaking mechanism. So that, the scalar sector of the Standard Model being trivial cannot give rise to the Bose-Einstein condensation. If this is the case, we should have free massless scalar particles. However, in Sect. 4 we will argue that, once the Higgs scalar fields are coupled to the gauge vector bosons of the Standard Model, then there are well-defined physical processes able to trigger the Higgs mechanism.

### 3 Comparison with non-perturbative numerical simulations

In the previous Section we have discussed in details two different approaches on spontaneous symmetry breaking for the one-component quantum scalar field theory. We have seen that these two approaches lead to sizeable differences that, in principle, can be tested by comparison with a truly non-perturbative approach to quantum scalar theories. Actually, the lattice approach to quantum field theories offers us the unique opportunity to study a quantum field theory by means of non-perturbative methods. To this end, firstly one needs to formulate the given quantum field theory in the Euclidean space by performing the analytic continuation to imaginary time. The technical convenience of considering field theories at purely imaginary times resides on the possibility to study a given quantum field theory by means of non-perturbative numerical techniques. In this respect it should be noticed that Osterwalder and Schrader established the complete equivalence between relativistic and Euclidean quantum field theories [24, 25]. In particular, the Osterwalder-Schrader positivity (also called reflection positivity) allows the reconstruction of the relativistic quantum theory from the Euclidean correlation functions (Schwinger function) and leads to a correspondence between the physical states of the real-time relativistic theory and the states obtained by acting with the Euclidean operators on the quantum vacuum.

Starting from the classical Lagrangian Eq.(2.1) one readily obtains the Euclidean action:

$$S_E = \int d^4x \mathcal{L}_E(x) = \int d^4x \left[ \frac{1}{2} (\partial_\mu \hat{\phi})^2 + \frac{1}{2} \mu^2 \hat{\phi}^2 + \frac{1}{4} \lambda_0 \hat{\phi}^4 \right]. \quad (3.1)$$

The Euclidean quantum field dynamics is dealt with from the functional integral point of view. In the lattice approach the Euclidean four-dimensional space-time is discretised to a hypercubic lattice with finite lattice spacing  $a$ , so that, in principle, the Schwinger functions can be evaluated by means of numerical functional integrations.

The lattice version of the Euclidean action Eq. (3.1) is written as:

$$S_E = a^4 \sum_x \left[ \frac{1}{2a^2} \sum_{\mu=1}^4 (\phi(x + a\hat{\mu}) - \phi(x))^2 + \frac{r_0}{2} \phi^2(x) + \frac{\lambda_0}{4} \phi^4(x) \right], \quad (3.2)$$

where  $x$  stands for a generic lattice site, and  $r_0$  and  $\lambda_0 > 0$  are free parameters. It is customary to adopt lattice units where  $a = 1$ .

In general, the continuum limit of the lattice theory  $a \rightarrow 0$  is obtained at a critical point of the lattice system where the dimensionless correlation length diverges. It turned out that <sup>3</sup>, for each given value of  $\lambda_0$ , there exists a critical value  $r_c(\lambda_0)$  such that the system is in the symmetric phase (vacuum expectation value of  $\phi$  vanishes) for  $r_0 > r_c(\lambda_0)$ , while it is in the broken phase (non-zero vacuum expectation value of  $\phi$ ) for  $r_0 < r_c(\lambda_0)$ . Remarkably, irrespective to the value of  $\lambda_0$ , the numerical simulations of the four-dimensional one-component scalar field theory on the lattice indicated that the continuum limit defines a trivial theory in both the symmetric and broken phases, in accordance with the recent rigorous result [8]. In other words, the continuous limit of the lattice theory is governed by the Gaussian fixed point  $\lambda^* = 0$ . Therefore, at the critical point of the model the critical exponents that characterise the singular behaviour of various quantities take the four-dimensional mean field values. In general, at a critical point the correlation length is much higher than the lattice spacing, so that one may send the lattice spacing to zero while keeping a fixed value for the physical mass parameter. In the scaling region, once the scale is set by the lattice spacing, all other parameters may then be expressed in terms of this scale parameter. Note, however, that all other physical parameters should scale correspondingly such that one can identify the correct continuum theory. This scaling regime may be observed quite early in the parameter space. Practically, the scaling region is characterised by a correlation length slightly higher than the lattice spacing. On the other hand, one has to be quite close to the critical point in order to observe the asymptotic scaling, namely how the lattice spacing tends to zero when  $\lambda \rightarrow \lambda^*$ . This asymptotic scaling is determined from the renormalisation group  $\beta$ -function.

The generally accepted assumption is that the renormalised perturbation theory is required to define the continuum limit. In this case, the asymptotic scaling is set by the two-loop perturbative  $\beta$ -function:

$$\beta_{pert}(\lambda) = \frac{9}{8\pi^2} \lambda^2 - \frac{51}{64\pi^4} \lambda^3. \quad (3.3)$$

Accordingly, the asymptotic scaling is governed by:

$$(am)_{pert} \sim \left( \frac{9}{8\pi^2} \lambda \right)^{\frac{17}{27}} \exp\left[ -\frac{8\pi^2}{9} \frac{1}{\lambda} \right]. \quad (3.4)$$

---

<sup>3</sup>A good account can be found in Ref. [26]

This scaling law is assumed to hold both in the symmetric phase [27] and in the broken phase [28]<sup>4</sup>. From Eq. (3.4) we see that in the continuum limit  $am \rightarrow 0$  the coupling constant  $\lambda$  is forced to go to zero. However, the ultraviolet cutoff  $\sim 1/a$  cannot be pushed to arbitrary high values due to the presence of a singularity (the Landau pole). Thus, we must admit that the continuum limit corresponds to  $m \rightarrow 0$ , i.e. the perturbative approach describes the triviality of the theory as an infrared Gaussian fixed point. Therefore, taking these results at face value, for fixed  $\lambda$  only at finite cutoff a non-vanishing value of  $\lambda$  is permitted. In this way within perturbation theory even a trivial theory may have an effective interaction below the cutoff.

On the other hand, in the broken phase the triviality and spontaneous symmetry breaking picture leads, according to Eq. (2.22), to the asymptotic scaling law:

$$(am)_{triv} \sim \exp\left[-\frac{8\pi^2}{9a_1} \frac{1}{\lambda}\right]. \quad (3.5)$$

This last equation shows that the continuous limit is an ultraviolet Gaussian fixed point leading to a free massive scalar field with mass finitely related to the condensate strength. In principle, the two different approaches to the spontaneous symmetry breaking for the one-component scalar field can be checked non perturbatively by direct lattice numerical simulations in a region of the coupling parameter space where the asymptotic scaling associated with the trivial Gaussian fixed point sets in. The first attempt in this direction was advanced in Refs. [29, 30] where it was numerically computed the effective potential on the lattice by employing the Euclidean action Eq. (3.2) with  $\lambda_0 = 0.5$ . The relevant lattice observables were the vacuum expectation value of the scalar field (also called the magnetisation):

$$v = \langle |\phi| \rangle \quad , \quad \phi \equiv \frac{1}{L^4} \sum_x \phi(x) \quad , \quad (3.6)$$

and the zero-momentum susceptibility:

$$\chi = L^4 [\langle |\phi|^2 \rangle - \langle |\phi| \rangle^2] \quad (3.7)$$

where  $L$  is the lattice linear size. The effective potential can be analysed in the lattice formulation by computing the vacuum expectation value of the field as a function of an uniform external source with strength  $J$ . Determining  $v(J)$  at several  $J$ -values is equivalent to invert the relation  $J = dV_{eff}/dv$  involving the effective potential  $V_{eff}(v)$ . As matter of fact, the one-loop potential agrees remarkably well with the lattice results, while its perturbative improvement fails to reproduce the Monte Carlo data. More precisely, in Refs. [29, 30] it was compared the two-loop renormalisation-group improved effective potential with the one in the triviality and spontaneous symmetry breaking picture discussed at length in Sec. 2. The numerical data significantly favour the unconventional interpretation of triviality over the conventional perturbative interpretation. However, it should be desirable to have a more direct test of the two asymptotic scaling laws. To this end, we note that in the critical region  $m^2 \sim \lambda_0 v^2$ . Therefore, according to Eqs. (3.4) and (3.5) we can write:

$$[\log(\lambda_0 v^2)]_{pert} \sim -\frac{16\pi^2}{9} \frac{1}{\lambda} + \frac{34}{27} \log\left(\frac{9}{8\pi^2} \lambda\right) + C_1 \quad , \quad (3.8)$$

---

<sup>4</sup>Note that the coupling constant  $g$  in the Lüscher and Weisz scheme is related to our  $\lambda$  by  $g = 6\lambda$ .

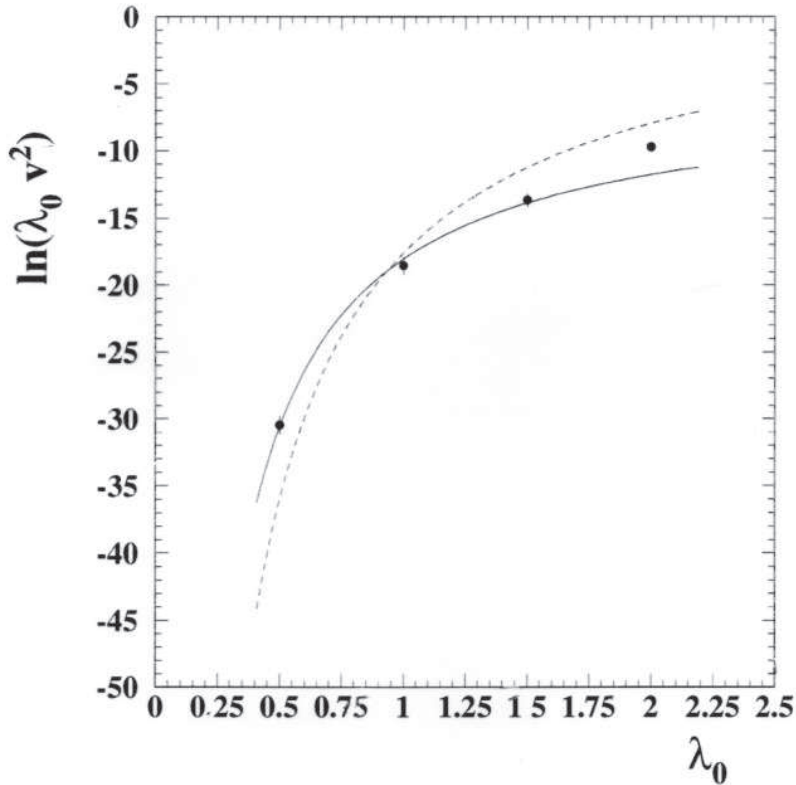


Figure 1: The lattice data for  $\ln(\lambda_0 v^2)$  for different values of  $\lambda_0$ . The continuous line corresponds to the best fit with Eq. (3.9), while the dashed line corresponds to the two-loop fit Eq. (3.8).

$$[\log(\lambda_0 v^2)]_{triv} \sim -\frac{16\pi^2}{9a_1} \frac{1}{\lambda} + C_2 \quad (3.9)$$

$C_1, C_2$  being some constant. Indeed, having at our disposal the vacuum expectation value of the scalar field for four different values of the coupling constant in the range  $0.5 \leq \lambda_0 \leq 2.0$ <sup>5</sup>, we tried to compare the two asymptotic scaling laws. In Fig. 1 we display the best fits to the numerical data with both Eqs. (3.8) and (3.9). Looking at Fig. 1 it is evident that the triviality scaling law compare to the data better than the two-loop scaling law. From the fit to the numerical data we inferred that:

$$a_1 = 1.18(7) . \quad (3.10)$$

Even though the above results are promising, it should be mentioned that at the the upper critical dimension ( $D=4$ ) the leading scaling behaviour for self-interacting scalar theory is coincident with mean field theory but, however, there are multiplicative logarithmic corrections that depend on the asymptotic scaling law. Unfortunately, for  $\lambda_0 \sim 1$  the numerical data do not show evidence of these logarithmic corrections (see Refs. [29, 30]). As a matter of fact, for a model-independent check of the asymptotic scaling law it would be desirable to have numerical data that display as clear as possible the effects of the logarithmic corrections to the mean-field scaling behaviour. Evidently, the logarithmic corrections are related to the non-Gaussian quantum fluctuations that, in turns, depend on the strength of the quartic self-coupling  $\lambda_0$ . For this reason it is customary to perform

<sup>5</sup>These results are based on a talk given by the author at the 15th International Symposium on Lattice Field Theory (Lattice 1997), Edinburgh, UK, July 22 - 26, 1997.

numerical simulations in the so-called Ising limit.

The Ising limit corresponds to  $\lambda_0 \rightarrow \infty$ . It is easy to see that, in this limit, the one-component scalar field theory becomes governed by the lattice action (see, eg, Ref. [27]):

$$S_{\text{Ising}} = -\kappa \sum_x \sum_{\mu} [\phi(x + \hat{\mu})\phi(x) + \phi(x - \hat{\mu})\phi(x)] \quad (3.11)$$

where  $\phi(x)$  takes only the values  $+1$  or  $-1$ . It is known that there is a critical coupling [31]:

$$\kappa_c = 0.074834(15) \quad (3.12)$$

such that for  $\kappa > \kappa_c$  the theory is in the broken phase, while for  $\kappa < \kappa_c$  it is in the symmetric phase. The continuum limit corresponds to  $\kappa \rightarrow \kappa_c$  where  $am \rightarrow 0$ .

As discussed in Section 2, the triviality of the scalar theory means that the renormalised self coupling vanishes as  $\frac{1}{\ln(\frac{\Lambda^2}{m_H^2})}$  when  $\Lambda \rightarrow \infty$ . Since on the lattice the ultraviolet cutoff is  $\Lambda = \frac{\pi}{a}$ , we have:

$$\lambda \sim \frac{1}{\ln(\frac{\Lambda}{m_H})} \sim \frac{1}{\ln(\frac{\pi}{am})} . \quad (3.13)$$

We have seen that the perturbative interpretation of triviality assumes that in the continuum limit there is an infrared Gaussian fixed point. On the other hand, according to Section 2, in the triviality and spontaneous symmetry breaking scenario the continuum dynamics is governed by an ultraviolet Gaussian fixed point. As we discuss below, these two different interpretation of triviality lead to different logarithmic correction to the Gaussian scaling laws that can be checked with numerical simulations on the lattice.

In Ref. [32, 33] extensive numerical lattice simulations of the one-component scalar field theory in the Ising limit have been performed using the Swendsen-Wang [34] and Wolff [35] cluster algorithms. According to the perturbative scheme one expects:

$$\lim_{\kappa \rightarrow \kappa_c^+} v^2 \chi \sim |\ln(\kappa - \kappa_c)| . \quad (3.14)$$

On the other hand, since in the triviality and spontaneous symmetry breaking scenario one expects that  $Z_\varphi \sim \ln(\frac{\Lambda}{m_H}) \sim |\ln(\kappa - \kappa_c)|$  we should have:

$$\lim_{\kappa \rightarrow \kappa_c^+} v^2 \chi \sim |\ln(\kappa - \kappa_c)|^2 . \quad (3.15)$$

The prediction in Eq. (3.15) can be directly compared with the lattice data reported in Ref. [32, 33]. Performing a fit to the lattice data with the functional form:

$$v^2 \chi = K |\ln(\kappa - \kappa_c)|^2 , \quad (3.16)$$

one obtains a rather good fit of the lattice data with [33]:

$$K = 0.07560(49) , \quad \kappa_c = 0.074821(12) , \quad \chi^2/dof \sim 1.0 . \quad (3.17)$$

The results of the fit are displayed in Fig. 2. Note that the precise determination of the critical coupling  $\kappa_c$  in Eq. (3.17) is in good agreement with Eq. (3.12).

On the other hand, the prediction based on 2-loop renormalised perturbation theory can be written as [36]:

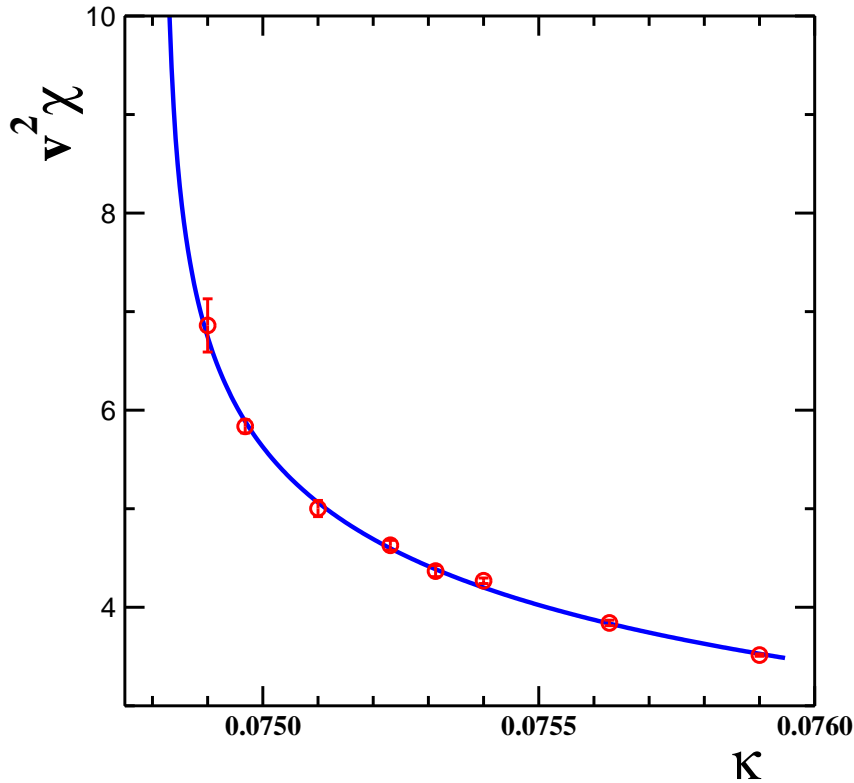


Figure 2: (Color online) Lattice data for  $v^2\chi$  versus  $\kappa$  together with the fit Eq. (3.16) (solid line).

$$[v^2\chi]_{pert} = A(l - \frac{25}{27}\ln l) + B \quad (3.18)$$

where  $l = |\ln(\kappa - \kappa_c)|$  and the constants  $A$  and  $B$  are constrained by the theoretical relations [27, 28]:

$$A = 1.20(3) \quad , \quad B = -1.6(5) \quad . \quad (3.19)$$

If one try to fit the data with Eq. (3.18) taking into account the constrains Eq. (3.19), then the resulting fit is rather poor (see the dashed line in Figure 1 of Ref. [33]):

$$A = 1.17 \quad , \quad B = -2.10 \quad , \quad \kappa_c = 0.074800(1) \quad , \quad \chi^2/dof \sim 10^2 \quad . \quad (3.20)$$

It should be mentioned that the above results have been subject to an intense debate in the literature (see, for instance, Refs. [37, 38] and references therein).

Aside from the previous evidences in favour of the triviality and spontaneous symmetry breaking proposal, further evidences would come from the direct detection of the increases of the condensate rescaling  $Z_\phi \sim |\ln(\kappa - \kappa_c)|$ . Indeed, observing that:

$$Z_\phi = 2 \kappa m^2 \chi \quad , \quad (3.21)$$

one can easily extract the condensate rescaling  $Z_\phi$  from the available lattice measurements. Here, in Fig. 3 we report the lattice data obtained in Ref. [32, 33] for  $Z_\phi$ , as defined in Eq. (3.21), versus  $am$  reported in Ref. [28]. For comparison we also report the wavefunction renormalisation constant of the fluctuating field  $Z_\eta$  taken from Ref. [28]. The lattice data are perfectly consistent with the logarithmic increases  $Z_\phi \sim \ln(\frac{1}{am})$  (see the dashed line in Fig. 3). These evidences for the non-trivial rescaling of the vac-



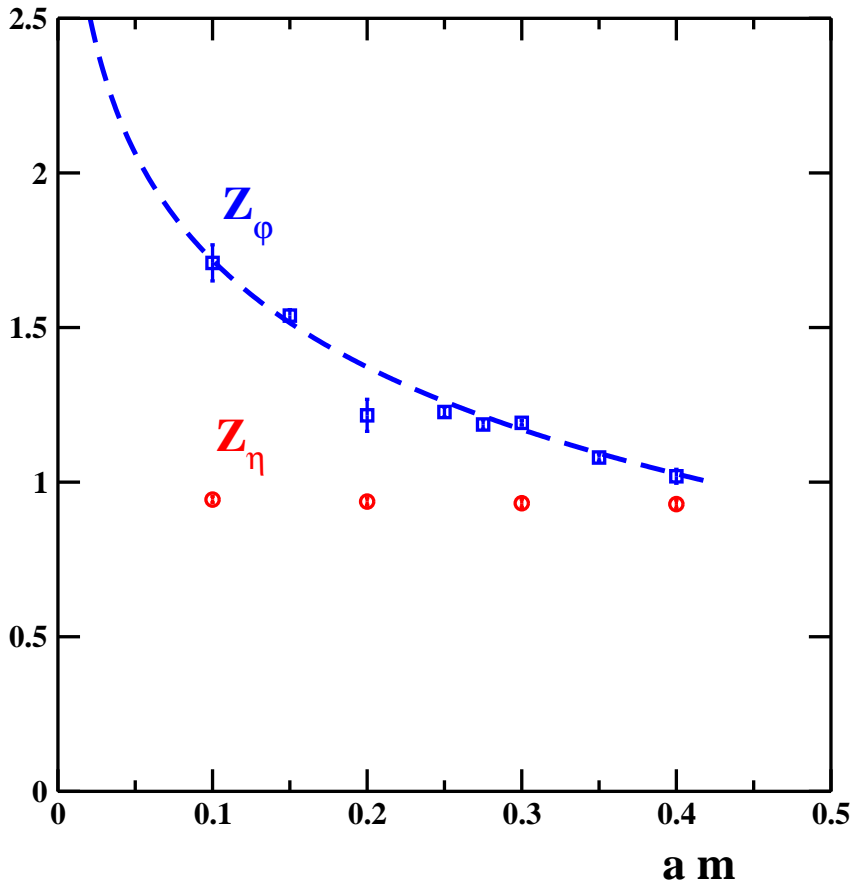


Figure 3: (Color online) The values of condensate rescaling  $Z_\phi$  and the wavefunction renormalisation constant  $Z_\eta$  versus  $am$ . The figure has been adapted from Fig. 2 of Ref. [33].

uum condensate has been criticised by the authors of Ref. [36]. In particular these authors claim that there are no evidences of a rescaling of the vacuum condensate that is different from the wavefunction renormalisation constant. However, they performed numerical simulations at two finite values of the quartic self-coupling  $\lambda_0 \sim 1$ . We already noticed that for  $\lambda_0 \sim 1$  there are no numerical evidences of the needed logarithmic corrections to the Gaussian mean field scaling laws. On the other hand, in the unique simulation at the Ising limit they measured the propagator in momentum space with lattice momenta  $\hat{p}^2$ , where  $\hat{p}_\mu = 2 \sin p_\mu/2$ . Previous studies indicated that the effects of the logarithmic increase of  $Z_\phi$  on the connected propagator manifest itself only at very small momenta  $\hat{p}^2 \lesssim 0.1$  (compare Fig. 3 with Fig. 4 in Ref. [32]). We suspect that the authors of Ref. [36] do not reach values of momenta very close to zero. Indeed, the wavefunction renormalisation constant reported in Table 5 of Ref. [36] agrees with the wavefunction renormalisation constant  $Z_\eta$  displayed in Fig. 3.

In the previous Section we have seen that, by adopting the alternative interpretation of triviality, the mass of the excitations over the vacuum condensate behave like a massive scalar field with mass  $m_H$  related to the renormalised vacuum condensate by Eq. (2.31). Using the lattice data one may easily estimate the numerical constant  $\xi$  in Eq. (2.31). Indeed, in Fig. 4, following the analyses reported in Ref. [33], we display  $m_H$  versus  $am$  together with our estimate of the extrapolated continuum limit obtained by assuming for the renormalised vacuum condensate the Standard Model value  $v \simeq 246$  GeV:

$$m_H = 750 \pm 30 \text{ GeV}, \quad (3.22)$$

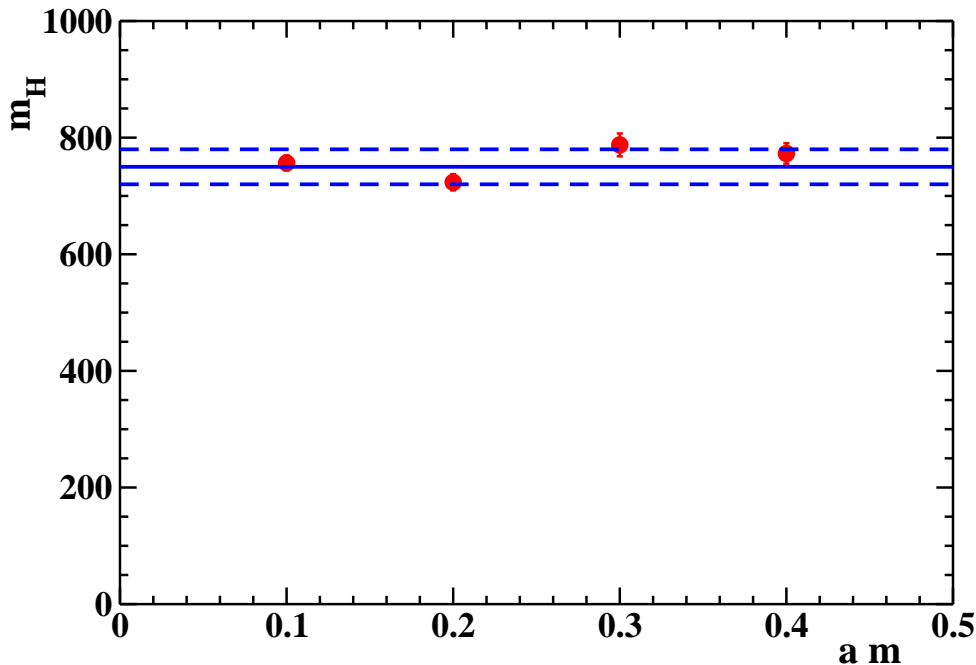


Figure 4: (Color online) The values of  $m_H$  obtained from the lattice data in Ref. [33] versus  $a m$  assuming  $v \simeq 246$  GeV. The horizontal lines correspond to Eq. (3.22).

where the displayed error includes both the statistical and systematic errors. In the next Section we shall see that the lattice estimate of the Higgs mass Eq. (3.22) is relevant for the physical Higgs boson of the Standard Model.

A further check of the asymptotic scaling laws can be obtained by means of the finite-size scaling theory derived using the renormalisation group methods [39, 40]. In the following we shall follow closely Ref. [41] where it is derived a finite-size scaling theory for the one-component scalar field theory in four dimensions.

Let us consider the partition functional  $Z[H, t]$  in presence of external sources:

$$S_{\text{Source}} = - \sum_x \left[ H(x) \phi(x) + \frac{1}{2} t(x) \phi^2(x) \right]. \quad (3.23)$$

Writing:

$$Z[H, t] = \exp\{ W[H, t] \}, \quad W[0, 0] = 0, \quad (3.24)$$

by a Legendre transformation of  $W[H, t]$  with respect to the external field  $H(x)$  one introduces the generating functional  $\Gamma[M, t]$  where:

$$M(x) = \frac{\delta W[M, t]}{\delta H(x)}. \quad (3.25)$$

The connected correlation functions can be obtained by functional derivatives of the generating functional  $\Gamma[M, t]$ :

$$\Gamma^{(K, N)}[y_1, \dots, y_K, x_1, \dots, x_N; M, t] = \frac{\delta^{K+N} \Gamma[M, t]}{\delta t(y_1) \dots \delta t(y_K) \delta M(x_1) \dots \delta M(x_N)}. \quad (3.26)$$

After renormalisation the renormalised connected correlation functions satisfy the renormalisation group equations that express the invariance of the physics under a rescaling  $\lambda$

of the mass parameter [39]. This allows one to examine the approach to criticality from within both the symmetric and the broken phases.

We know that in the renormalised perturbation approach the critical point is a Gaussian infrared fixed point. The relevant flow equations are:

$$\begin{aligned} \lim_{\lambda \rightarrow 0} \frac{g_R(\lambda)}{g_R} &\sim \frac{2}{3g_R} \frac{1}{|\ln \lambda|} && \text{pert.} \\ \lim_{\lambda \rightarrow 0} \frac{t(\lambda)}{t} &\sim \left[ \frac{2}{3} \frac{1}{|\ln \lambda|} \right]^{\frac{1}{3}} && \text{pert.} \\ \lim_{\lambda \rightarrow 0} \frac{M(\lambda)}{M} &\sim 1 && \text{pert.} \end{aligned} \quad (3.27)$$

where  $g_R(1) = g_R$ ,  $t(1) = t$ ,  $M(1) = M$ . On the other hand, in the triviality and spontaneous symmetry breaking picture there is a ultraviolet Gaussian fixed point. In this case the flow equations are <sup>6</sup>:

$$\begin{aligned} \lim_{\lambda \rightarrow 0} \frac{g_R(\lambda)}{g_R} &\sim \frac{2}{3a_1g_R} \frac{1}{|\ln \lambda|} && \text{triv.} \\ \lim_{\lambda \rightarrow 0} \frac{t(\lambda)}{t} &\sim \left[ \frac{2}{3a_1} \frac{1}{|\ln \lambda|} \right]^{\frac{1}{3a_1}} && \text{triv.} \\ \lim_{\lambda \rightarrow 0} \frac{M(\lambda)}{M} &\sim 1 && \text{triv.} \end{aligned} \quad (3.28)$$

The renormalisation constants of the infinite-volume theory render finite the finite-volume theory too. As a consequence the renormalisation group equations for the finite-volume theory are the same as in the case of infinite volume. This allows to develop a finite-size scaling theory for the model under study. Actually, we are interested in the correlation function  $\Gamma_R^{(0,0)}$ . In the renormalised perturbation theory one readily obtain [41]:

$$\Gamma_R^{(0,0)} \sim \Gamma_R^{(0,0)} \left[ L^2 t \left( \frac{2}{3g_R \ln L} \right)^{\frac{1}{3}}, LM, \frac{2}{3 \ln L} \right] + \frac{3}{4} \left( \frac{2}{3g_R} \right)^{\frac{2}{3}} t^2 (\ln L)^{\frac{1}{3}} \quad \text{pert.} \quad (3.29)$$

where  $L$  is the linear extent of the system. In the triviality picture we have:

$$\Gamma_R^{(0,0)} \sim \Gamma_R^{(0,0)} \left[ L^2 t \left( \frac{2}{3a_1g_R \ln L} \right)^{\frac{1}{3a_1}}, LM, \frac{2}{3a_1 \ln L} \right] + \frac{3a_1}{4} \left( \frac{2}{3a_1g_R} \right)^{\frac{2}{3a_1}} t^2 (\ln L)^{1 - \frac{2}{3a_1}} \quad \text{triv.} \quad (3.30)$$

Since in both approaches the renormalised coupling is small, perturbation theory may be applied to calculate  $\Gamma_R^{(0,0)}$ :

$$\Gamma_R^{(0,0)} \simeq [g_R M^4 + t M^2], \quad (3.31)$$

so that:

$$\Gamma_R^{(0,0)} \sim c_1 t M^2 (\ln L)^{-\frac{1}{3}} + c_2 M^4 (\ln L)^{-1} + c_3 t^2 (\ln L)^{\frac{1}{3}} \quad \text{pert.} \quad (3.32)$$

---

<sup>6</sup>In perturbation theory the quantum phase transition at the critical point is continuous. In the triviality and spontaneous symmetry breaking picture the order of the transition is not known. The phase transition could well be first order. However, numerical simulations on the lattice indicated that the phase transition is almost continuous. In other words, if the transition is first order, then it must be a weak first-order phase transition.

$$\Gamma_R^{(0,0)} \sim c_1 t M^2 (\ln L)^{-\frac{1}{3a_1}} + c_2 M^4 (\ln L)^{-1} + c_3 t^2 (\ln L)^{1-\frac{2}{3a_1}} \quad \textit{triv.} \quad (3.33)$$

Since

$$H(x) = \frac{\delta \Gamma[M, t]}{\delta M(x)}, \quad (3.34)$$

we readily obtain:

$$H \simeq c_4 t M (\ln L)^{-\frac{1}{3}} + c_5 M^3 (\ln L)^{-1} \quad \textit{pert.} \quad (3.35)$$

$$H \simeq c_4 t M (\ln L)^{-\frac{1}{3a_1}} + c_5 M^3 (\ln L)^{-1} \quad \textit{triv.} \quad (3.36)$$

So that the free energy density in presence of an external field is:

$$W_L(t, H) \simeq c'_1 t M^2 (\ln L)^{-\frac{1}{3}} + c'_2 M^4 (\ln L)^{-1} + c_3 t^2 (\ln L)^{\frac{1}{3}} \quad \textit{pert.} \quad (3.37)$$

$$W_L(t, H) \simeq c'_1 t M^2 (\ln L)^{-\frac{1}{3a_1}} + c'_2 M^4 (\ln L)^{-1} + c_3 t^2 (\ln L)^{1-\frac{1}{3a_1}} \quad \textit{triv.} \quad (3.38)$$

where  $M$  is related to  $H$  by Eqs. (3.35) and (3.36) respectively.

If  $H = 0$ , from Eqs. (3.35) and (3.36) we infer:

$$M^2 \simeq t (\ln L)^{\frac{2}{3}} \quad \textit{pert.} \quad (3.39)$$

and

$$M^2 \simeq t (\ln L)^{1-\frac{1}{3a_1}} \quad \textit{triv.} \quad (3.40)$$

Thus:

$$W_L \simeq t^2 (\ln L)^{\frac{1}{3}} \quad \textit{pert.} \quad (3.41)$$

and

$$W_L \simeq t^2 (\ln L)^{1-\frac{2}{3a_1}} \quad \textit{triv.} \quad (3.42)$$

Finally, for the specific heat one gets:

$$C_L \simeq (\ln L)^{\frac{1}{3}} \quad \textit{pert.} \quad (3.43)$$

and

$$C_L \simeq (\ln L)^{1-\frac{2}{3a_1}} \quad \textit{triv.} \quad (3.44)$$

In general, the critical behaviour of Ising-type systems can be analysed through its partition function zeroes. The study of partition function zeroes was initiated by Yang and Lee. The Lee-Yang theorem states that for ferromagnetic systems all of the zeroes of the partition function in the external magnetic field lie on the imaginary axis for real temperatures. Fisher was the first to analyse the zeroes in the complex temperature plane. Therefore, the partition function zeroes in the temperature plane are referred to as Fisher zeroes, while those in the complex plane of external fields as Lee-Yang zeroes. The finite-size scaling theory allow to determine the logarithmic corrections to the zeroes of the partition function. The total free energy at the critical temperature in presence of an external field is given by Eqs. (3.37) and (3.38):

$$F_L(t = 0, H) \simeq c'_2 M^4 L^4 (\ln L)^{-1} \quad \textit{pert. \& triv.} \quad (3.45)$$

where, from Eqs. (3.35) and (3.36) at  $t = 0$  we have:

$$H \simeq c_5 M^3 (\ln L)^{-1} \quad \textit{pert. \& triv.} \quad (3.46)$$

Whereupon we obtain:

$$F_L(t=0, H) \sim H^{\frac{4}{3}} L^4 (\ln L)^{\frac{1}{3}} \quad \textit{pert. \& triv.} \quad (3.47)$$

The partition function is therefore:

$$Z_L(t=0, H) = Q(H^{\frac{4}{3}} L^4 (\ln L)^{\frac{1}{3}}) \quad \textit{pert. \& triv.} \quad (3.48)$$

From this last equation it follows that, if at some value of H the partition function vanishes, then:

$$H^{\frac{4}{3}} = L^{-4} (\ln L)^{-\frac{1}{3}} Q^{-1}(0) \quad \textit{pert. \& triv.} \quad (3.49)$$

or

$$H_j \sim L^{-3} (\ln L)^{-\frac{1}{4}} \quad \textit{pert. \& triv.} \quad (3.50)$$

where  $j$  indicates the index of the zero. For the Fisher zeroes, we note that from Eqs. (3.35) and (3.36) for  $H = 0$  one obtains for the total free energy:

$$F_L(t, H=0) \sim L^4 t^2 (\ln L)^{\frac{1}{3}} \quad \textit{pert.} \quad (3.51)$$

$$F_L(t, H=0) \sim L^4 t^2 (\ln L)^{1-\frac{2}{3a_1}} \quad \textit{triv.} \quad (3.52)$$

Therefore, if the partition function, which is the exponential of the free energy, vanishes, then for the  $j$ th zero:

$$R_j^{-1}(0) = L^4 t^2 (\ln L)^{\frac{1}{3}} \quad \textit{pert.} \quad (3.53)$$

$$R_j^{-1}(0) = L^4 t^2 (\ln L)^{1-\frac{2}{3a_1}} \quad \textit{triv.} \quad (3.54)$$

As a consequence we have:

$$t_j \sim L^{-2} (\ln L)^{-\frac{1}{6}} \quad \textit{pert.} \quad (3.55)$$

$$t_j \sim L^{-2} (\ln L)^{-\frac{1}{2}+\frac{1}{3a_1}} \quad \textit{triv.} \quad (3.56)$$

We now want to compare the finite-size analysis to existing numerical calculations in the literature for both asymptotic scaling laws. In the broken phase we have only found numerical simulations dealing with the finite-size analysis for the zeroes of the partition function and the specific heat. In the case of the Lee-Yang zeroes Ref. [42] reports the following measured exponent of the logarithmic corrections:

$$\alpha_{meas} = -0.248(17) \quad \textit{Lee-Yang zeroes} \quad (3.57)$$

For the Fischer zeroes Ref. [41] reports:

$$\begin{aligned} \alpha_{meas} &= -0.217(12) \quad 8 \leq L \leq 24 \quad \textit{Fisher zeroes} \\ \alpha_{meas} &= -0.21(4) \quad 12 \leq L \leq 24 \quad \textit{Fisher zeroes} \end{aligned} \quad (3.58)$$

In the case of the Lee-Yang zeroes both scaling laws give  $\alpha_{theor} = -1/4$  in excellent agreement with the measured exponent Eq. (3.57). On the other hand, for the Fisher zeroes, using Eqs. (3.55), (3.56) and (3.10) we have:

$$\begin{aligned} \alpha_{theor} &= -\frac{1}{6} \simeq -0.167 \quad \textit{Fisher zeroes} \quad \textit{pert.} \\ \alpha_{theor} &= -\frac{1}{2} + \frac{1}{3a_1} \simeq -0.217(17) \quad \textit{Fisher zeroes} \quad \textit{triv.} \end{aligned} \quad (3.59)$$

From this last equation we see that the triviality and spontaneous symmetry breaking scaling law is in excellent agreements with the numerical outcomes, while the two-loop perturbative approach displays a sizeable deviation of at least two standard deviations. Finally, in Ref. [43] the four-dimensional Ising model is studied to probe the possibility of observing in Monte Carlo simulations the logarithmic corrections to the mean-field theory near criticality. In particular, by fitting the specific heat  $C_L$  as some power of  $\ln L$ , the authors of Ref. [43] reported:

$$\alpha_{meas} = 0.37(9) \quad 6 \leq L \leq 14 \quad \text{specific heat} \quad (3.60)$$

On the other hand, from Eqs. (3.43) and (3.44) we infer:

$$\begin{aligned} \alpha_{theor} &= \frac{1}{3} \simeq 0.333 && \text{specific heat} && \textit{pert.} \\ \alpha_{theor} &= 1 - \frac{2}{3a_1} \simeq 0.435(11) && \text{specific heat} && \textit{triv} \end{aligned} \quad (3.61)$$

From these equations we see that both the triviality and spontaneous symmetry breaking and the two-loop perturbative scaling laws are in agreements with the numerical simulation results.

To summarise, we have shown that the triviality and spontaneous symmetry breaking picture compares remarkably well to several results from non-perturbative numerical simulations. On the contrary, the two-loop renormalised perturbative approach suffers from serious discrepancies with respect to numerical outcomes in the broken phase of the lattice implementation of the one-component scalar field theory. These results shed doubts on the widely accepted opinion that the perturbative approach to the Higgs mechanism is fully supported by precise non-perturbative numerical simulations.

## 4 The quantum liquid picture

In the previous Sections we have discussed at length the one-component quantum scalar field with quartic self-interaction. Actually, the scalar sector of the Standard Model involves four quantum scalar fields arranged in a weak doublet:

$$\hat{\Phi}(x) = \begin{pmatrix} \frac{\hat{\phi}_1(x) + i\hat{\phi}_2(x)}{\sqrt{2}} \\ \frac{\hat{\phi}_3(x) + i\hat{\phi}_4(x)}{\sqrt{2}} \end{pmatrix}. \quad (4.1)$$

Therefore the Lagrangian of the Standard Model scalar sector is assumed to be:

$$\mathcal{L}_{scalar} = \partial_\mu \hat{\Phi}^\dagger \partial^\mu \hat{\Phi} - \mu^2 \hat{\Phi}^\dagger \hat{\Phi} - \lambda_0 (\hat{\Phi}^\dagger \hat{\Phi})^2 \quad (4.2)$$

with a tachyonic mass term  $\mu^2 < 0$  and a positive quartic self-coupling  $\lambda_0 > 0$ . Evidently the Lagrangian Eq. (4.2) corresponds to a  $O(4)$ -symmetric self-interacting scalar field theory. As compared to the one-component model, the solution of the  $O(n)$ -symmetric model is not much more difficult. In the broken symmetry phase, the presence of (massless) Goldstone bosons for  $n > 2$  gives rise to a number of complications. Nevertheless, it has been well established by numerical simulations the triviality of the  $O(4)$  symmetric model in the broken phase (see Ref. [44] and references therein). The emerging physical

picture of the  $O(4)$  model thus obtained is practically the same as for the one-component model treated earlier. In particular, as in the one-component model, the triviality of the theory does not allow us to implement the spontaneous symmetry breaking mechanism and, as a result of the triviality, we should end with four massless scalar fields. Fortunately the scalar fields of the Standard Model are also coupled to the gauge vector bosons of the electroweak gauge group  $SU(2) \otimes U(1)$ . This is easily accomplished by replacing in Eq. (4.2) the derivatives  $\partial_\mu$  with the covariant derivatives  $D_\mu$ . However, in the absence of gauge fixing, a local gauge symmetry cannot break spontaneously, as we know from Elitzur's theorem [45]. As a consequence, to enforce the symmetry breaking of the gauge symmetries we are forced to make a gauge choice. Since the physics cannot depend on the gauge fixing, we are free to adopt the physical gauge where three scalar fields are gauged away (unitary gauge). As a consequence the quantum scalar fields Eq. (4.1) can be written as:

$$\hat{\Phi}(x) = \begin{pmatrix} 0 \\ \frac{\hat{\phi}(x)}{\sqrt{2}} \end{pmatrix} \quad (4.3)$$

where  $\hat{\phi}(x)$  is a one-component quantum scalar field. We see, thus, that the Lagrangian Eq. (4.2) reduces to the Lagrangian in Eq. (2.1). As discussed in Sect. 2, to trigger the spontaneous symmetry breaking we need some amount of non-Gaussian fluctuations in the scalar quantum vacuum. Again we face with the problem that, within the pure scalar sector, we do not have a physical mechanism to generate a positive self-coupling needed to trigger the Bose-Einstein condensation of the quantum scalar field. Actually, in Ref. [22] we showed that the interactions of the scalar field  $\hat{\phi}$  with vector bosons and fermion fields of the standard Model will induce an effective positive scalar self-coupling  $\lambda_{eff}$  whose scale evolution is governed by the running coupling constants  $g(\mu), g'(\mu), \lambda_f(\mu)$ , where  $g$  is the  $SU(2)$  gauge coupling,  $g'$  the  $U(1)$  gauge coupling and  $\lambda_f(\mu)$  indicates the generic coupling of  $\hat{\phi}$  to the fermion fields. We are led, then, to the following effective scalar Lagrangian:

$$\mathcal{L} = \frac{1}{2} (\partial_\mu \hat{\phi})^2 - \frac{1}{4} \lambda_{eff} \hat{\phi}^4. \quad (4.4)$$

We have already seen that the presence of a positive quartic self-coupling, irrespective to the actual value of the self-coupling, leads to the Bose-Einstein condensation of the scalar field  $\hat{\phi}$ :

$$\hat{\phi}(x) = \hat{H}(x) + v \quad (4.5)$$

characterised by a finite scalar condensate  $v$  and a massive quantum scalar field  $H(x)$  (the Higgs field) with mass finitely related to the condensate strength. The strength of the condensate is an arbitrary parameter of the theory. Once identified  $v$  with the Standard Model condensate strength,  $v \simeq 246$  GeV, the mass of the fluctuating Higgs field has been estimated by precise non-perturbative numerical simulation, Eq. (3.22). As a matter of fact, a more precise value of the Higgs field has been obtained in Ref. [46] where, for the first time, it was enlightened in the preliminary LHC Run 2 data some evidences of a rather broad resonance structure around 700 GeV consistent with a heavy Higgs boson. According to Ref. [46], in the following we shall assume:

$$m_H \simeq 730 \text{ GeV} \quad (4.6)$$

that, by the way, is fully consistent with the lattice determination, Eq. (3.22).

We have reached the remarkable result that the massless quantum scalar fields of the

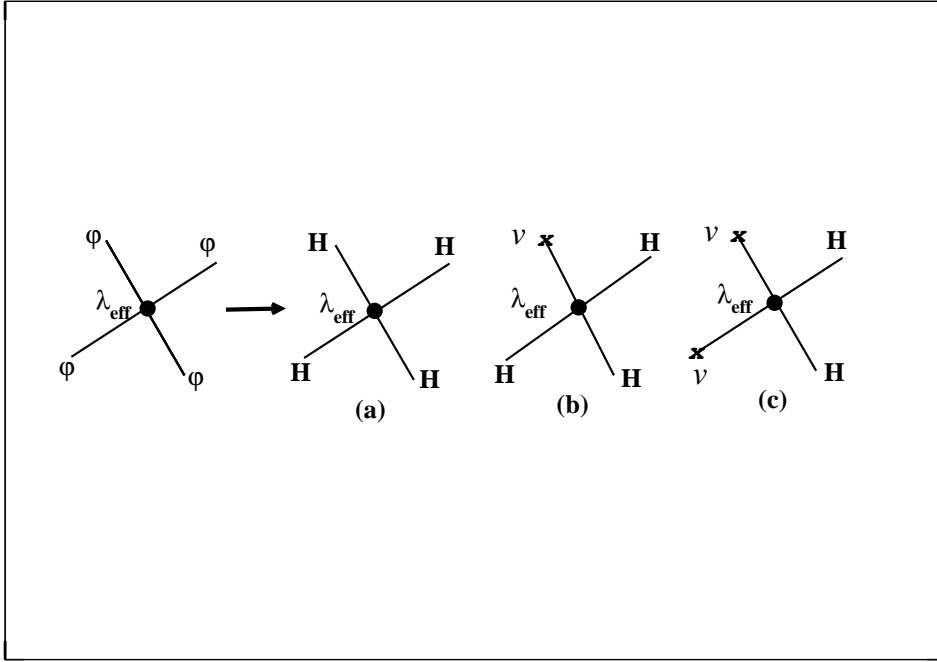


Figure 5: Self-couplings of the H scalar field.

Standard Model, once coupled to the gauge vector bosons and fermions, undergoes dynamically the Bose-Einstein condensation needed to implement the Higgs mechanism. Note that in our approach we are not invoking the unphysical Mexican-hat classical potential. The symmetry breaking mechanism is generated by non-Gaussian fluctuations in the scalar quantum vacuum generated by a positive quartic self-coupling. Since our mechanism does not depend on the actual value of the positive quartic self-coupling, we see that there is no stability problem for the vacuum condensation. On the other hand, it should be clear that our  $\lambda_{eff}$  is not washed out by the scalar quantum fluctuations since the scale evolution is dictated by the renormalisation group evolution of the gauge and Yukawa couplings. Actually, it is known that the scale evolution of  $\lambda_{eff}$  dictates that the quartic self-coupling becomes negative at some high-energy scale  $\Lambda_{eff} \sim 10^{10}$  GeV. This means that our mechanism can be realised only if  $v \lesssim \Lambda_{eff}$ , condition amply satisfied in the Standard Model.

Up to now we have found that the triviality and spontaneous symmetry breaking picture leads in the Standard Model to the scalar Bose-Einstein condensation giving rise to an almost free massive scalar fluctuating Higgs field  $\hat{H}$  with a rather large mass given by Eq. (4.6). This picture is modified substantially by the presence of a small positive quartic self-coupling [22]. In fact, the quartic self-coupling, after taking into account Eq. (4.5), leads to new interacting terms for the Higgs field. In Fig. 5 we show how the self-coupling generates new interaction terms for the Higgs field. Actually in Fig. 5 we are not displaying the interaction term linear in  $\hat{H}$ . Indeed, since the fluctuating quantum field  $\hat{H}$  involves only modes with  $\vec{k} \neq 0$ , this term vanishes. There is a further term proportional to  $v^4$  that merely adds a contribution to the vacuum energy density that, now, is given by:

$$\mathcal{E} \simeq -\frac{m_H^4}{128\pi^2} + \frac{\lambda_{eff}}{4} v^4. \quad (4.7)$$



In Ref. [22] we argued that  $\lambda_{eff} \lesssim \lambda_{SM}$ , where  $\lambda_{SM}$  is the quartic self-coupling in the standard perturbative approach with the Mexican-hat classical potential. So that the vacuum energy density in Eq. (4.7) is still negative.

Looking at Fig. 5 we see that the Higgs field acquires quartic and cubic self-interaction terms. There is a further interaction term quadratic in the Higgs field. This quadratic term implies that the Higgs field may undergo interactions with the vacuum condensate that generate a new coherent propagating condensate excitations with mass:

$$m_h^2 \sim \lambda_{eff} v^2 \sim 10^2 \text{ GeV} . \quad (4.8)$$

In Ref. [22] this condensate excitation was identified with the new LHC scalar resonance with mass 125 GeV. This lead us to look at the Higgs condensate as a quantum liquid analogous to the Bose-Einstein condensate in superfluid He II. Indeed, the low-lying excitations of the Higgs condensate resembled two Higgs bosons that correspond to the relativistic version of the phonons and rotons in superfluid He II. In the dilute gas approximation, that is the relevant regime for the LHC physics, these excitations of the Higgs condensate behave as two Standard Model Higgs bosons denoted with  $h$  and  $H$  respectively. The light Higgs boson has a mass given by Eq. (4.8), while the mass of the heavy Higgs boson is given by Eq. (4.6). Note that the mass of the  $h$  Higgs boson is naturally related to the weak scale  $v \sim 10^2$  GeV, i.e. there is no naturalness problem, namely we do not need the fine tuning of any parameter to obtain a mass of order  $10^2$  GeV.

We would like to emphasise that we are not saying that there are two different elementary quantum Higgs fields. On the contrary, we have a unique local quantum Higgs field. However, since the scalar condensate behaves like the He II quantum liquid, when the Higgs field acts on the condensate it can give rise to two elementary excitations, namely the phonon-like and roton-like excitations corresponding to long-range collective and localised disturbances of the condensate, respectively. These elementary condensate excitations behave as weakly interacting scalar fields with vastly different mass. These two Higgs bosons will interact with the gauge vector bosons. We already pointed out [22] that the couplings of the Higgs condensate elementary excitations to the gauge vector bosons are fixed by the gauge symmetries. As a consequence, both the Higgs bosons  $h$  and  $H$  will be coupled to gauge bosons as in the usual perturbative approximation of the Standard Model.

As concern the coupling to fermion fields, if we admit the presence of the Yukawa terms in the Lagrangian, then we are led to an effective Yukawa lagrangian:

$$\mathcal{L}_Y^{eff}(x) = \sqrt{Z_{wf}^h} \frac{\lambda_f}{\sqrt{2}} \hat{\psi}_f(x) \hat{\psi}_f(x) \hat{h}(x) + \sqrt{Z_{wf}^H} \frac{\lambda_f}{\sqrt{2}} \hat{\psi}_f(x) \hat{\psi}_f(x) \hat{H}(x) , \quad (4.9)$$

where  $\hat{\psi}_f(x)$  indicates a generic fermion quantum field and the Yukawa coupling satisfies the usual relation:

$$\lambda_f = \frac{\sqrt{2} m_f}{v} . \quad (4.10)$$

In Eq. (4.9)  $Z_{wf}^h$  and  $Z_{wf}^H$  are wavefunction renormalisation constant that, roughly, take care of the eventual mismatch in the overlap between the fermion and quasiparticle wavefunctions. In Ref. [22] we were able to fix these constants from a comparison with the experimental observations. As a result we argued that:

$$Z_{wf}^h \simeq 1 \quad , \quad Z_{wf}^H \simeq \frac{m_h}{m_H} \simeq 0.171 . \quad (4.11)$$

A notable consequence of Eq. (4.11) is that our light Higgs boson  $h$  is practically indistinguishable from the perturbative Higgs boson.

## 5 Comparison with experimental observations

Once established that the perturbations of the scalar condensate due to the quantum Higgs field behave as two independent weakly interacting massive scalar fields, we need to investigate the experimental signatures and the interactions of these Higgs condensate elementary excitations. Obviously, the most striking consequence of our approach is the prevision of an additional heavy Higgs boson. As we already said, the light Higgs boson is the natural candidate for the new LHC scalar resonance at 125 GeV. On the other hand, our previous phenomenological analysis of the preliminary LHC Run 2 data in the golden channel [46] hinted at the presence of a broad scalar resonance with central mass of 730 GeV. The aim of this Section is to present the comparison of our theoretical proposal to the experimental observations from both the ATLAS and CMS LHC Collaborations based on the full Run 2 datasets. Considering that our light Higgs boson  $h$  is practically indistinguishable from the perturbative Higgs boson, we shall restrict ourself to the heavy Higgs boson  $H$ .

The phenomenological signatures of a massive Higgs boson are determined by the couplings with the gauge and fermion fields of the Standard Model. As already argued in Sect. 4, the couplings of the Higgs field to the gauge vector bosons are dictated by the gauge symmetries, so that the couplings of the  $H$  Higgs boson to the gauge vector bosons are the same as in perturbation theory notwithstanding the non-perturbative scalar condensation driving the spontaneous breaking of the gauge symmetries. The unique difference arises from the Yukawa coupling to the fermions. Given the rather large mass of the  $H$  Higgs boson, the only relevant Yukawa coupling is the coupling to the top quark. According to Eq. (4.9) the top Yukawa coupling of the  $H$  Higgs boson is suppressed by a factor  $\sqrt{Z_{wf}^H}$  with respect to perturbation theory.

The Higgs boson can be produced in many different ways. In general, there are four common ways to produce the Higgs boson in proton-proton colliders: gluon-gluon fusion, vector-boson fusion, associated production with a vector boson and associated production with a pair of top quarks. However, the main production mechanisms are by gluon-gluon fusion and vector-boson fusion. Therefore, in the following we shall restrict ourself to these production mechanisms. To evaluate the Higgs event production at LHC we need the inclusive Higgs production cross section. Observing that the couplings of the  $H$  boson to vector bosons are the same as those of a Standard Model Higgs boson, the  $H$  boson production cross section by vector-boson fusion is the same as in the perturbative Standard Model calculations. On the other hand, for the gluon-gluon fusion production mechanism, considering that the gluon coupling to the Higgs boson in the Standard Model is mediated mainly by triangular loops of top and bottom quarks, it follows that the inclusive production cross section is given by the Standard Model cross section suppressed by a factor  $Z_{wf}^H$ . Therefore, within our approximations, the total inclusive cross section for the production of the  $H$  Higgs boson we can write:

$$\sigma(pp \rightarrow H) \simeq \sigma_{VBF}(pp \rightarrow H) + \sigma_{GGF}(pp \rightarrow H), \quad (5.1)$$

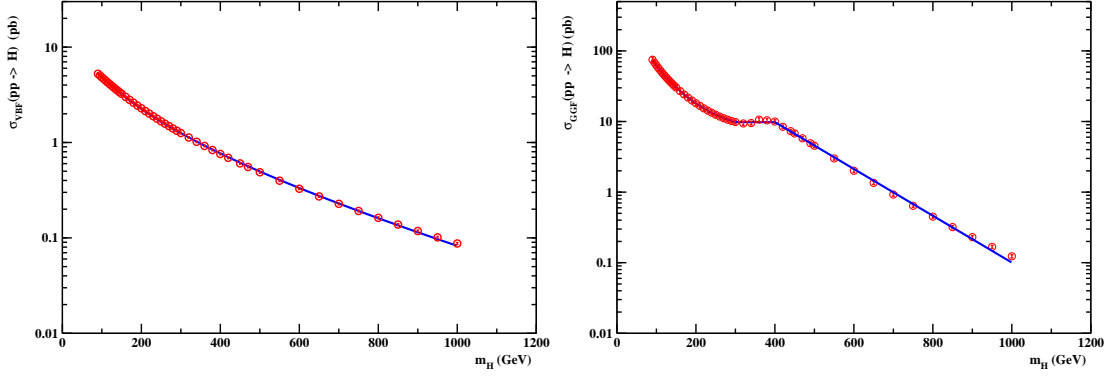


Figure 6: (Color online) Inclusive H Higgs boson production cross sections for the VBF processes (left panel) and GGF processes (right panel) at  $\sqrt{s} = 13$  TeV. The data points have been taken from Ref. [47]. The (blue) continuous lines correspond to Eqs. (5.2) and (5.4) respectively.

where  $\sigma_{VBF}$  and  $\sigma_{GGF}$  are the vector-boson fusion and gluon-gluon fusion inclusive cross sections, respectively. In the Standard Model the calculations of the cross sections computed at next-to-next-to-leading and next-to-leading order for a high mass Higgs boson with Standard Model-like couplings at  $\sqrt{s} = 13$  TeV are provided by the LHC Higgs Cross Section Working Group [47]. As concern the Standard Model gluon-gluon fusion cross section we found [46] that this cross section can be usefully interpolated by (see Fig. 6, right panel):

$$\sigma_{GGF}^{SM}(p p \rightarrow H) \simeq \begin{cases} \left( \frac{a_1}{m_H} + a_2 m_H^3 \right) \exp(-a_3 m_H) & m_H \leq 300 \text{ GeV} \\ a_4 & 300 \text{ GeV} \leq m_H \leq 400 \text{ GeV} \\ a_4 \exp[-a_5(m_H - 400 \text{ GeV})] & 400 \text{ GeV} \leq m_H \end{cases} \quad (5.2)$$

where  $m_H$  is expressed in GeV and:

$$\begin{aligned} a_1 &\simeq 1.24 \cdot 10^4 \text{ pb GeV} \quad , \quad a_2 \simeq 1.49 \cdot 10^{-6} \text{ pb GeV}^{-3} \quad , \\ a_3 &\simeq 7.06 \cdot 10^{-3} \text{ GeV}^{-1} \quad , \quad a_4 \simeq 9.80 \text{ pb} \quad , \\ a_5 &\simeq 7.63 \cdot 10^{-3} \text{ GeV}^{-1} \quad . \end{aligned} \quad (5.3)$$

Likewise the Standard Model vector-boson fusion cross section can be parametrised as (see Fig. 6, left panel):

$$\sigma_{VBF}^{SM}(p p \rightarrow H) \simeq \left( b_1 + \frac{b_2}{m_H} + \frac{b_3}{m_H^2} \right) \exp(-b_4 m_H) \quad , \quad (5.4)$$

with:

$$\begin{aligned} b_1 &\simeq -2.69 \cdot 10^{-6} \text{ pb} \quad , \quad b_2 \simeq 8.08 \cdot 10^2 \text{ pb GeV} \quad , \\ b_3 &\simeq -1.98 \cdot 10^4 \text{ pb GeV}^2 \quad , \quad b_4 \simeq 2.26 \cdot 10^{-3} \text{ GeV}^{-1} \quad . \end{aligned} \quad (5.5)$$

We would like to stress that in theoretical calculations of the production cross section, in the mass range relevant to us, there is a typical  $\pm 5\%$  uncertainty due to the choice of the parton distributions, the QCD scale and the strong interaction coupling. In the

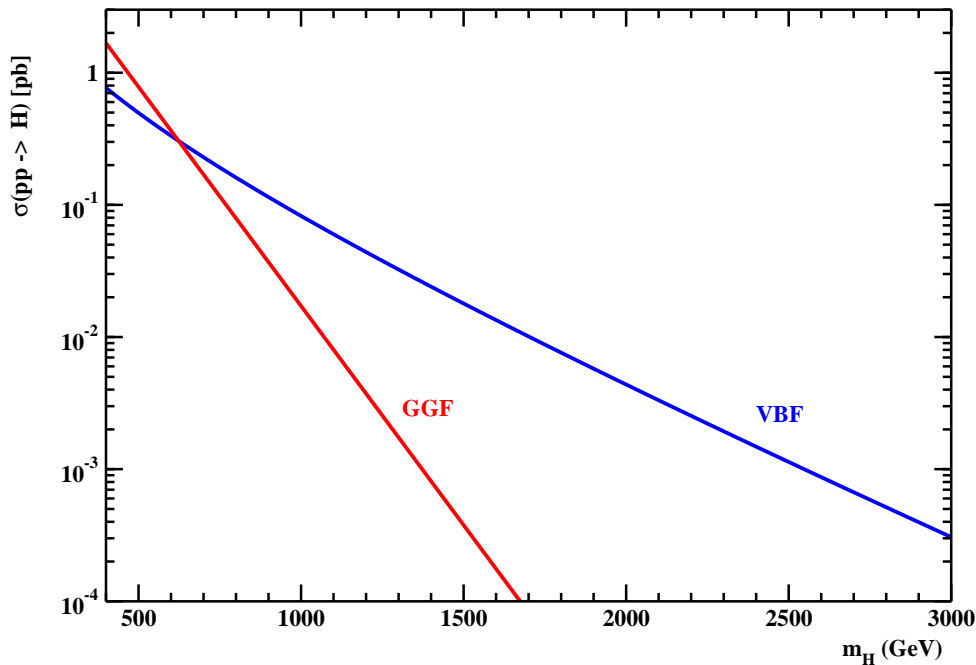


Figure 7: (Color online) Inclusive H Higgs boson production cross sections for the VBF processes (blue continuous line) and GGF processes (red continuous line) as a function of  $m_H$  at  $\sqrt{s} = 13$  TeV.

following, usually, we will not take into account these theoretical uncertainties. Our previous discussion lead us to assume that to a good approximation we can write:

$$\sigma_{VBF}(pp \rightarrow H) \simeq \sigma_{VBF}^{SM}(pp \rightarrow H) \quad , \quad \sigma_{GGF}(pp \rightarrow H) \simeq Z_{wf}^H \sigma_{GGF}^{SM}(pp \rightarrow H) \quad . \quad (5.6)$$

In Fig. 7 we compare the VBF and GGF production cross sections given by Eq. (5.6) after taking into account the value of  $Z_{wf}^H$  in Eq. (4.11). It is evident that the main production mechanism of the heavy H Higgs boson is by the VBF processes since at  $m_H \simeq 730$  GeV it results:

$$\sigma_{VBF}(pp \rightarrow H) \simeq 2 \sigma_{GGF}(pp \rightarrow H) \quad . \quad (5.7)$$

In order to determine the phenomenological signatures of the massive H Higgs boson we need to examine the decay modes. Given the rather large mass of the heavy Higgs boson, the main decay modes are the decays into two massive vector bosons (see, e.g., Refs. [48, 49]):

$$\Gamma(H \rightarrow W^+ W^-) \simeq \frac{G_F m_H^3}{8\pi\sqrt{2}} \sqrt{1 - \frac{4m_W^2}{m_H^2}} \left( 1 - 4 \frac{m_W^2}{m_H^2} + 12 \frac{m_W^4}{m_H^4} \right) \quad (5.8)$$

and

$$\Gamma(H \rightarrow Z^0 Z^0) \simeq \frac{G_F m_H^3}{16\pi\sqrt{2}} \sqrt{1 - \frac{4m_Z^2}{m_H^2}} \left( 1 - 4 \frac{m_Z^2}{m_H^2} + 12 \frac{m_Z^4}{m_H^4} \right) \quad . \quad (5.9)$$

The couplings of the H Higgs boson to the fermions are given by the Yukawa couplings. As we said before, for heavy Higgs the only relevant fermion coupling is the top Yukawa

coupling. The width for the decays of the H boson into a  $t\bar{t}$  pairs is easily found [48, 49]:

$$\Gamma(H \rightarrow t\bar{t}) \simeq Z_{wf}^H \frac{3 G_F m_H m_t^2}{4\pi \sqrt{2}} \left(1 - 4 \frac{m_t^2}{m_H^2}\right)^{\frac{3}{2}}. \quad (5.10)$$

Obviously, there are several other decay modes that, however, are expected to be negligible. So that, to a good approximation, the heavy Higgs boson total width is given by:

$$\Gamma_H \simeq \Gamma(H \rightarrow W^+ W^-) + \Gamma(H \rightarrow Z^0 Z^0) + \Gamma(H \rightarrow t\bar{t}). \quad (5.11)$$

We see that almost all the decay modes are given by the decays into  $W^+W^-$  and  $Z^0Z^0$ . Moreover we have:

$$Br(H \rightarrow W^+W^-) \simeq 2 Br(H \rightarrow Z^0Z^0). \quad (5.12)$$

The above discussion show that our heavy Higgs boson is a rather broad resonance with a total width  $\Gamma_H$  that is about 30 % of its mass. This poses challenging theoretical problem in dealing with a resonance with such a huge width. A convenient way is to use the Breit-Wigner formula [50] to model the resonance in terms of the physical mass and width. More precisely, in the resonance rest frame we may estimate the probability to find the H resonance in the energy interval  $(E, E + dE)$  by means of the modified Lorentzian distribution:

$$L_H(E) \simeq \frac{1}{1.0325 \pi} \frac{\frac{\Gamma_H(E)}{2}}{\left(E - 730 \text{ GeV}\right)^2 + \left(\frac{\Gamma_H(E)}{2}\right)^2}, \quad (5.13)$$

where  $\Gamma_H(E)$  is given by Eq. (5.11), and the normalisation is such that:

$$\int_0^\infty L_H(E) dE = 1. \quad (5.14)$$

Note that, in the limit  $\Gamma_H \rightarrow 0$ ,  $L_H(E)$  reduces to  $\delta(E - 730 \text{ GeV})$ .

In general, we are interested in collider processes  $pp \rightarrow H \rightarrow X$ . In particular, we wish to estimate the invariant mass spectrum of the particles produced in the Higgs decays. Let  $N_H(E_1, E_2)$  be the number of events produced by the H Higgs decays in the energy interval  $(E_1, E_2)$ . Then, we have:

$$N_H(E_1, E_2) \simeq \mathcal{L} \int_{E_1}^{E_2} \sigma(pp \rightarrow H) Br(H \rightarrow X) \varepsilon(E) L_H(E) dE, \quad (5.15)$$

where  $\mathcal{L}$  is the integrated luminosity. The parameter  $\varepsilon(E)$  accounts for the efficiency of trigger, acceptance of the detectors, the kinematic selections, and so on. In general,  $\varepsilon(E)$  is expected to depend on the energy, the selected channel and the detector. The above approximations should furnish a reasonable estimate of the invariant mass distribution for values of the invariant mass  $M$  in a range  $\Delta M \sim 10^2 \text{ GeV}$  around  $m_H$ .

## 5.1 Comparison with the ATLAS Run 2 datasets

In the present Section we intend to contrast our theoretical proposal of an additional Standard Model heavy Higgs boson to the experimental outcomes from the LHC ATLAS Collaboration. Actually, in a recent paper [51] we attempted a comparison of our proposal

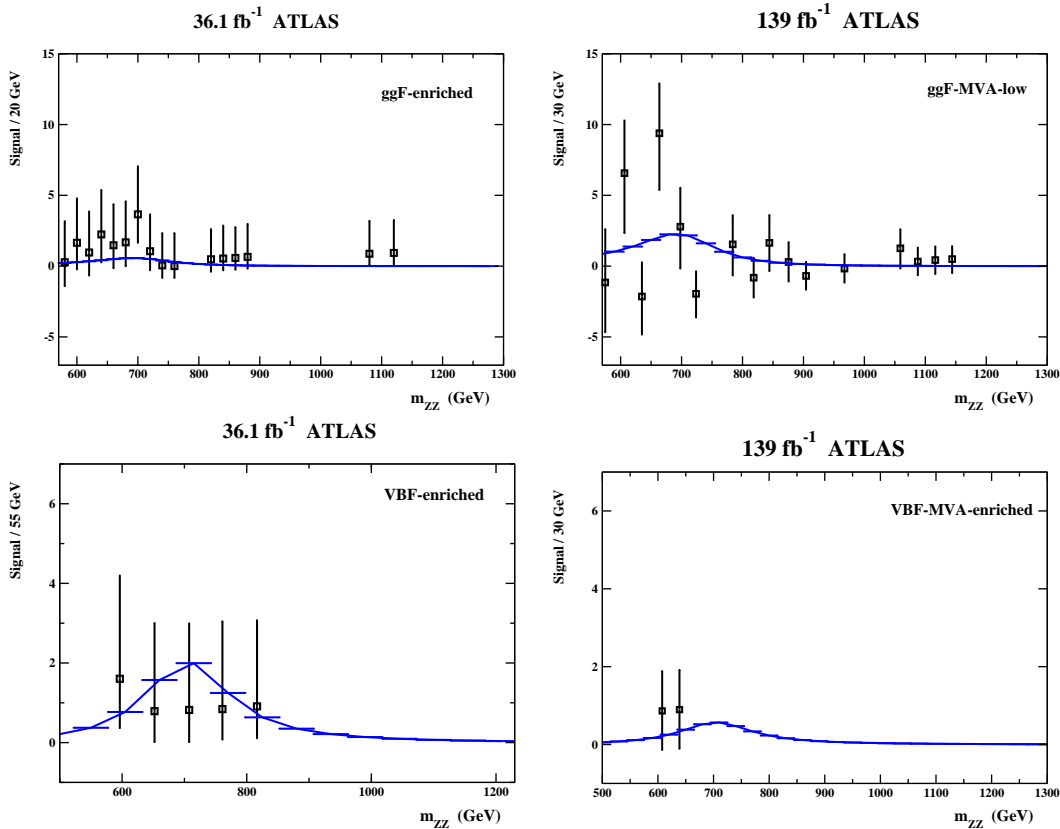


Figure 8: (Color online) Signal distributions versus the invariant mass  $m_{ZZ}$  in the high-mass region  $m_{ZZ} \gtrsim 600$  GeV for the GGF and VBF processes with integrated luminosity  $36.1 fb^{-1}$  and  $139 fb^{-1}$ . The (blue) continuous lines are the expected theoretical distributions for the H Higgs boson.

to the ATLAS full Run 2 datasets in the main decay channels  $H \rightarrow WW, ZZ$ . As concern the decays  $H \rightarrow ZZ$  in the golden channel here we merely restrict ourself to a summary of Ref. [51]. To this end, let us consider the golden channel  $H \rightarrow ZZ \rightarrow \ell^+ \ell^- \ell^+ \ell^-$ ,  $\ell$  being an electron or a muon. It is well established that the golden channel has very low branching ratio, nevertheless the presence of leptons allows to efficiently reduce the huge background mainly due to diboson production. Indeed, the four-lepton channel, albeit rare, has the clearest and cleanest signature of all the possible Higgs boson decay modes due to the small background contamination. Since it is assumed that an additional Higgs boson would be produced predominantly via gluon-gluon fusion (GGF) and vector-boson fusion (VBF) processes, the events are classified into GGF and VBF categories and results are interpreted separately for the GGF and VBF production modes. A search for a new high-mass resonance decaying into electron or muon pairs has been performed the ATLAS experiment using data collected at  $\sqrt{s} = 13$  TeV corresponding to an integrated luminosity of  $36 fb^{-1}$  [52] and upgraded to  $139 fb^{-1}$  [53]. In order to be sensitive to the VBF production mode, for the  $36.1 fb^{-1}$  data set, the ATLAS Collaboration [52] classified the events into four categories, namely one for the VBF production mode and three for the GGF production mode. If an event has two or more jets with  $p_T$  greater than 30 GeV, with the two leading jets  $j_1, j_2$  well separated in the pseudo-rapidity  $\eta$ , i.e.  $|\eta_{j_1, j_2}| > 3.3$ , and having an invariant mass  $m_{j_1, j_2} > 400$  GeV, then this event is classified into the VBF-enriched category. Otherwise the event is classified into one of the GGF-enriched categories. Such classification is used only in the search for a heavy scalar produced within the narrow width approximation. On the other hand, for the full Run 2 data set the event

classification targeting different production processes has been optimised using machine learning algorithms [53]. More precisely, to improve the sensitivity in the search of a heavy Higgs signal produced either in the VBF or in the GGF production mode, it was used two classifiers, a VBF classifier and a GGF classifier. These classifiers were built with deep neural networks. The networks were trained by means of simulated signal events from a heavy Higgs boson with masses ranging from 200 GeV up to 1400 GeV in the narrow width approximation, and from the Standard Model continuous  $ZZ$  background.

In Fig. 8, adapted from Figs. 2 and 5 of Ref. [51], we show the signal invariant-mass distribution for the golden channel for the GGF category corresponding to  $36 \text{ fb}^{-1}$  (upper left panel) and  $139 \text{ fb}^{-1}$  (upper right panel) and VBF category ( $36 \text{ fb}^{-1}$  bottom left panel,  $139 \text{ fb}^{-1}$  bottom right panel) in the high invariant mass region  $m_{ZZ} \gtrsim 600 \text{ GeV}$ . The signal distributions can be easily obtained by subtracting from the event distributions the irreducible  $ZZ$  backgrounds that constitute the main source of the Standard Model background in the high invariant-mass region. We, also, compare in Fig. 8 the observed signal distributions to our theoretical proposal obtained by means of Eq. (5.15). For the 2016 ATLAS data set, we see that the expected signal histogram is perfectly compatible with the data, but it is evident that the integrated luminosity is too low to claim an evidence of our heavy Higgs boson. As concern the full data set, for the comparison we have taken into account that the selection cuts applied by the ATLAS Collaboration to the full Run 2 data set are more stringent with respect to the preliminary data. As a consequence, the resulting efficiency to detect a high-mass broad resonance is drastically reduced. This lead us to argue that there was not enough sensitivity to detect the expected signal at least in this channel (this last point is thoroughly discussed in Ref. [51]).

According to Eq. (5.12) the main decay mode of our heavy Higgs boson is the decays into two  $W$  vector bosons. Thus, the most stringent constraints should arise from the experimental searches for a heavy Higgs boson decaying into two  $W$  gauge bosons. In fact, in our previous paper [22] we compared our theoretical expectations to the search for neutral heavy resonances in the  $WW \rightarrow e\nu\mu\nu$  decay channel performed by the ATLAS Collaboration using proton-proton collision data at  $\sqrt{s} = 13 \text{ TeV}$  and corresponding to an integrated luminosity of  $36.1 \text{ fb}^{-1}$  [52]. In Ref. [51] we analysed the full Run 2 dataset presented by the ATLAS Collaboration [54] on the search of heavy resonances decaying into two vector bosons  $WW$ ,  $ZZ$  or  $WZ$  using collected data corresponding to an integrated luminosity of  $139 \text{ fb}^{-1}$ . Actually, in Ref. [54] the research focused on a heavy neutral scalar resonance, called the Radion, which appears in some theoretical models and which, indeed, can decay into  $WW$  or  $ZZ$  with a branching ratio approximatively given by Eq. (5.12). Moreover, the Radion-like scalar resonances couple to the Standard Model fermions and gauge bosons with strengths similarly to a heavy Higgs boson. Considering that these heavy scalar resonances have a rather narrow widths, in our previous paper [51] we considered the observed limits on the production processes presented in Ref. [54] as indicative of the production of a heavy Standard Model heavy Higgs boson in the narrow width approximation. Since recently the ATLAS Collaboration has presented the results of a search for heavy neutral Higgs-like resonances decaying into two  $W$  bosons, which subsequently decay into the  $e\nu\mu\nu$  final state [55], it is worthwhile here to compare our theoretical proposal with these experimental outcomes from the ATLAS experiment.

In Fig. 9, adapted from Fig. 7 of Ref. [55], we display the observed limits at 95 % confidence level on a heavy Higgs-like boson production cross section times the branching fraction  $Br(H \rightarrow WW)$  for both the gluon-gluon fusion and vector-boson fusion produc-

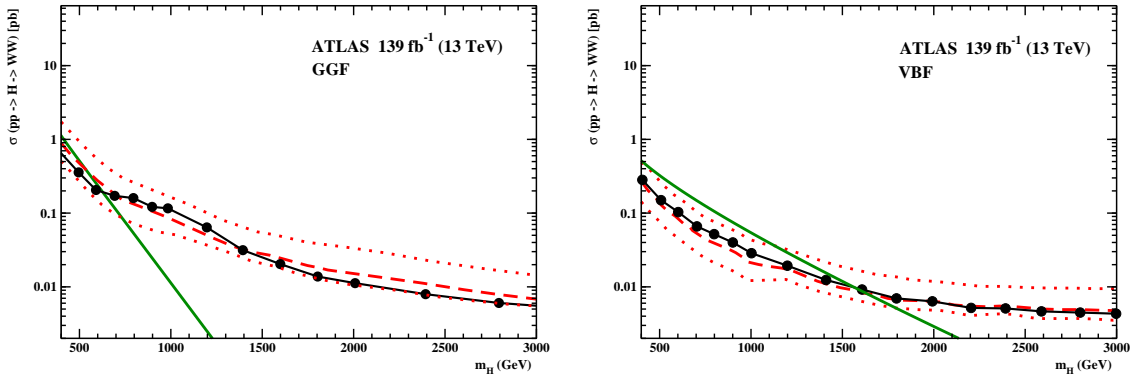


Figure 9: (Color online) Limits on the GGF (left panel) and VBF (right panel) production cross sections times the branching fraction for the processes  $pp \rightarrow H \rightarrow WW$ . Full circles represent the observed signal, the (red) dashed lines are the expected signal, while the (red) dotted lines demarcate the 95 % confidence level regions of the expected background. The continuous (green) lines are our theoretical estimate for the gluon-gluon fusion and vector-boson fusion production cross sections times the branching ratio  $\text{Br}(H \rightarrow WW)$ .

tion mechanisms in the narrow width approximation. We also display our estimate for the product of the gluon-gluon fusion and vector-boson fusion production cross sections times the branching ratio for the decay of the H Higgs boson into two vector W bosons. In the comparison of our theoretical results with the observed limits one should keep in mind that the narrow width approximation adopted by the ATLAS Collaboration amounts to set the decay width of the heavy scalar to be much smaller than the detector resolution and the our branching ration for the decay  $H \rightarrow WW$  is slightly higher than the one obtained within the usual perturbative approximation with the classical Mexican-heat Higgs potential. As a consequence the experimental limits become somewhat weaker in the case our heavy Higgs broad resonance. Looking at Fig. 9 it is evident that, in the case of the gluon-gluon production mechanism our theoretical cross section is still compatible with the observed limits in the relevant mass range. As concern the vector-boson production mechanism, we see that our theoretical estimate of the production cross sections times the branching ratio  $\text{Br}(H \rightarrow WW)$  stays higher than the observed limits in the high-mass region of interest. Even taking into account the previous caveats, we see that at best our theoretical results are compatible with the ATLAS data at the 95 % confidence level.

To conclude the present Section, we can affirm that the LHC full Run 2 datasets from the ATLAS Collaboration did not display a clear evidence for an additional heavy Higgs boson. Even though we already argued [51] that probably there is not enough sensitivity, mainly due to the severe selection cuts, to detect the expected signal especially in the vector-boson fusion production mechanism, we must admit that the absence of experimental evidences of an additional heavy Higgs boson from the ATLAS experimental results looks problematic. We shall further discuss this point after the comparison with the data collected from the CMS experiment.

## 5.2 Comparison with the CMS Run 2 datasets

The complete Run 2 datasets released by the LHC CMS Collaboration correspond to an integrated luminosity of about  $138 \text{ fb}^{-1}$ . In our previous paper [46] we found some evidence of a broad scalar resonance that looks consistent with our Standard Model heavy



Higgs boson in the golden channel based on the preliminary Run 2 data collected by the CMS Collaborations corresponding to an integrated luminosity of  $77.4 \text{ fb}^{-1}$ . Nevertheless, observing that the main decay mode of a heavy Higgs boson is the decays into two W vector bosons, the lack of experimental evidences in this decay channel posed challenging problems to our theoretical proposal. In fact, we were well aware that in absence of convincing experimental signatures in the decay channel  $H \rightarrow WW$  would lead us to reject the heavy Higgs boson proposal. Fortunately, the recent paper Ref. [56], where the CMS Collaboration presented a search for a high mass resonance decaying into a pair of W bosons using the full data recorded by CMS during the LHC Run 2 and corresponding to an integrated luminosity of  $138 \text{ fb}^{-1}$ , we found some evidences for a broad resonance that resembled a heavy Higgs boson [57].

The aim of the present Section is to compare our theoretical proposal for an additional heavy Higgs boson to the full Run 2 datasets released by the CMS Collaboration in the main decay channels  $H \rightarrow WW, ZZ$ .

Concerning the heavy Higgs decay into two W vector bosons, we shall follow closely our recent paper Ref [57]. The CMS Collaboration presented a search for a high mass resonance decaying into a pair of W bosons, using the full data set recorded by CMS during the LHC Run 2 corresponding to an integrated luminosity of  $138 \text{ fb}^{-1}$ . The search strategy for  $H \rightarrow W^+W^-$  was based on the final state in which both W bosons decay leptonically, resulting in a signature with two isolated, oppositely charged, high  $p_T$  leptons (electrons or muons) and large missing transverse momentum, due to the undetected neutrinos. So that, the bulk of the signal comes from direct W decays to electrons or muons of opposite charge. However, even if not explicitly mentioned in Ref. [56], the small contributions proceeding through an intermediate  $\tau$  lepton are implicitly included. Therefore, in Ref. [56] it is always included the W boson decays into all three lepton types, such as the  $\ell$  symbol in  $W \rightarrow \ell + \nu$  comprises all three leptons  $e, \mu, \tau$ . To increase the signal sensitivity, it were used a event categorisation optimised for the gluon-gluon fusion and vector-boson fusion production mechanisms. Accordingly, it was introduced a parameter  $f_{VBF}$  corresponding to the fraction of the VBF production cross section with respect to the total cross section. As a result,  $f_{VBF} = 0$  corresponds to GGF production signal while  $f_{VBF} = 1$  considers only the VBF production signal. For a heavy scalar resonance with Standard Model-like couplings  $f_{VBF}$  was set to the expectation using the cross sections provided by the LHC Higgs Cross Section Working Group [47].

The results were presented as upper limits on the product of the cross section with the relevant branching ratio on the production of a high mass scalar resonance. The 68 % and 95 % confidence level upper limits on  $\sigma(pp \rightarrow H \rightarrow WW \rightarrow 2\ell 2\nu)$  are displayed in Fig. 4 of Ref. [56] for four different scenarios,  $f_{VBF} = 0$ ,  $f_{VBF} = 1$ , floating  $f_{VBF}$  and Standard Model  $f_{VBF}$ . Interestingly enough, the CMS Collaboration reported an excess of data over the Standard Model background expectations for heavy Higgs boson masses ranging in the interval 600 GeV - 1000 GeV. Moreover, the largest localised excess in the data over the background were observed in the VBF production mechanism near 650 GeV with a local significance of about 3.8 standard deviations. Note, however, that due to the large fraction of missing energy from the neutrinos, the resolution on the mass is still quite broad. As a consequence, the excess is compatible with a resonant signal with mass ranging from roughly 600 GeV to 1000 GeV.

To be concrete, in order to compare with our theoretical expectations in Fig. 10 we report  $\sigma(pp \rightarrow H \rightarrow WW \rightarrow 2\ell 2\nu)$  as a function of the Higgs mass  $m_H$  in the case of a heavy

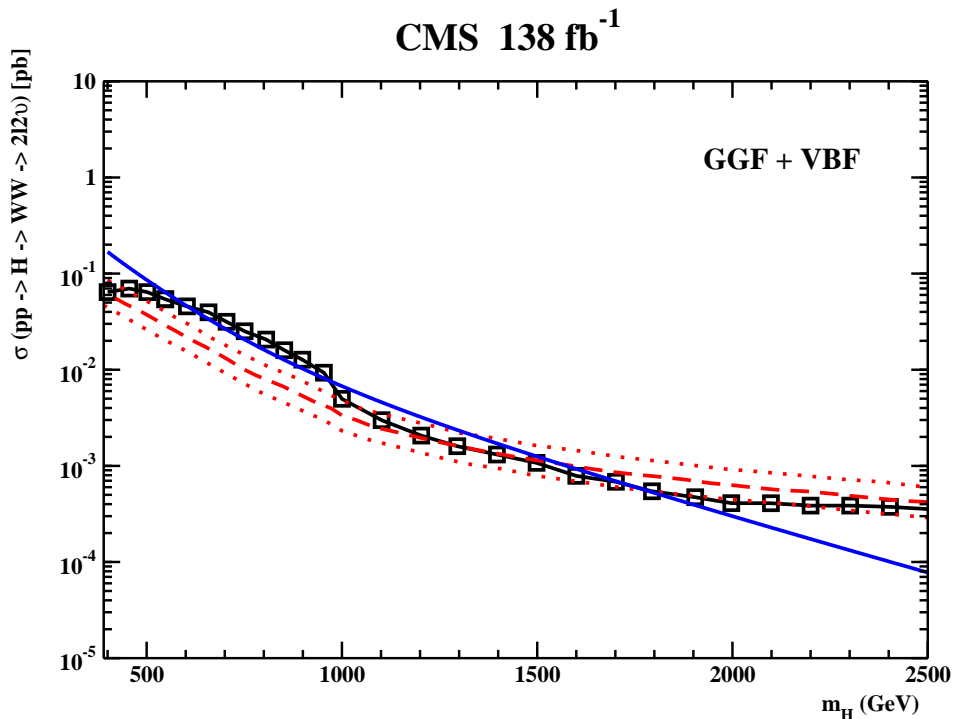


Figure 10: (Color online) Product of the cross section  $\sigma(pp \rightarrow H)$  with the branching ratio  $Br(H \rightarrow WW \rightarrow 2\ell 2\nu)$  for the search of a Standard Model heavy Higgs boson versus the Higgs mass  $m_H$ . The data have been adapted from Fig. 4, bottom right panel, of Ref. [56]. Black squares correspond to the observed signal, the (red) dashed line is the expected Standard Model background together with the 68 % CL limits (red dotted lines). The full (blue) line corresponds to the product of the cross section times the branching ratio for our heavy Higgs boson.

scalar resonance with Standard Model-like couplings (Standard Model  $f_{VBF}$ ). Looking at Fig. 10 it is evident that the observed signals display a sizeable broad excess with respect to expected Standard Model signal in the mass range 600 GeV - 800 GeV. Clearly, these excesses cannot be accounted for by a heavy scalar resonance with a narrow width. In addition, for a heavy Standard Model Higgs boson the main production mechanism would be by gluon-fusion processes for  $m_H \lesssim 1000$  GeV, so that the resulting production cross section would lead to a signal greater by at least a factor of two with respect to the observed signal (see red line in Fig. 4, bottom right panel, of Ref. [56]). On the other hand, in our theoretical proposal the heavy Standard Model Higgs boson has a rather large width implying that the expected signal extends on the mass range 600 GeV - 800 GeV with a broad peak around  $m_H \simeq 700$  GeV. Moreover, we already argued that the main production mechanism is by vector-boson fusion since the gluon-gluon fusion processes are strongly suppressed (see Fig. 7). To be quantitative, using Eq. (5.6) for the cross section and Eqs. (5.8) - (5.11) to evaluate the relevant branching ratio, we may easily estimate the inclusive production cross section for our heavy Higgs boson in the given channels. The result, displayed in Fig. 10, seems to compare reasonable well to the observed signal in the relevant Higgs mass range  $600 \text{ GeV} \lesssim m_H \lesssim 800 \text{ GeV}$ . It should be emphasised that the rejection of the background-only hypothesis in a statistical sense will depend, in general, on the plausibility of the new signal hypothesis and the degree to which it can describe the data. In this respect, the presence of a rather broad excess around  $m_H \simeq 700$  GeV is perfectly consistent with the fact that our Standard Model heavy Higgs boson has

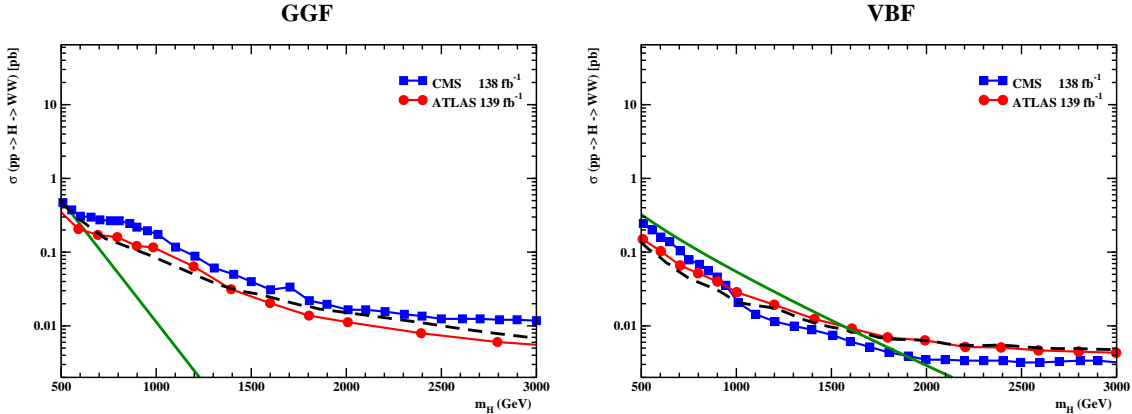


Figure 11: (Color online) Limits on the GGF (left panel) and VBF (right panel) production cross sections times the branching fraction for the processes  $pp \rightarrow H \rightarrow W$ . Full (red) circles represent the observed signal from ATLAS, full (blue) squares correspond to the observed signal from CMS. The (black) dashed lines are the expected signal from ATLAS. The continuous (green) lines are our theoretical estimate for the gluon-gluon fusion and vector-boson fusion production cross sections times the branching ratio  $\text{Br}(H \rightarrow WW)$ .

a central mass at  $m_H \simeq 730$  GeV and a huge width. Moreover, we have estimated that the cumulative effects of the excesses in the mass range 600 GeV - 800 GeV reach a statistical significance well above five standard deviations even including the look elsewhere effect [58]. The look elsewhere effect takes into account that, when searching for a new resonance somewhere in a possible mass range, the significance of observing a local excess of events must take into account the probability of observing such an excess anywhere in the range. Note, however, that for a broad resonance this effect should not matter due to the fact that statistical fluctuations over an extended mass range are practically never realised. It is necessary to mention that the agreement of our theoretical estimates with the observed production cross section limits depends crucially on the circumstance that our heavy Higgs boson  $H$  is produced mainly by the vector boson fusion mechanism and that the main decay modes are the decays into two massive gauge vector bosons.

This preliminary evidence of a broad scalar resonance from the CMS observations looks encouraging. However, we have said in the previous Section that the full Run 2 datasets from the ATLAS Collaboration data did not displayed experimental evidences of an additional heavy Higgs boson notwithstanding both experiments used a comparable integrated luminosity. To better elucidate this last point, it is useful to directly compare the limits on the GGF and VBF production cross sections times the branching fraction for the processes  $pp \rightarrow H \rightarrow WW$  reported by the two experiments.

In Fig. 11 we display the limits on the gluon-gluon fusion (left panel) and vector-boson fusion(right panel) production cross sections times the relevant branching fraction reported from ATLAS and CMS experiments. For the CMS limits we used:

$$\text{Br}(WW \rightarrow \ell\nu\ell\nu) \simeq 0.103, \quad \ell = e, \mu, \tau. \quad (5.16)$$

Figure 11 show clearly that in the mass range 600 GeV - 800 GeV the CMS limits stay above the ones from the ATLAS by about a factor of two. In our opinion these discrepancies arise from the circumstance that the tight selection cuts adopted by the ATLAS Collaboration resulted in a smaller sensitivity for the search of a broad scalar resonance in the mass range relevant to us. Obviously, it goes without saying that this

matter can be elucidated only by the experimental collaborations.

We are well aware that the above preliminary experimental evidences of the H Higgs boson are not enough to claim the experimental discovery of a new particle. Fortunately we have at our disposal the already mentioned evidence of a broad scalar resonance that looks consistent with the heavy Higgs boson in the golden channel based on the preliminary Run 2 data collected by the CMS collaborations [46]. It is useful to summarise the strategy we followed in Ref. [46]. Firstly, in Fig. 12, upper panel, we reproduce the distribution of the four-lepton reconstructed invariant mass  $m_{4\ell}$  for the golden channel in the full mass range presented by the CMS Collaboration by combining the 2016 and 2017 CMS data [59] and corresponding to an integrated luminosity of  $77.4 \text{ fb}^{-1}$ . From the full range distribution we extracted the invariant mass distribution with bin size 4 GeV in the high-mass region  $m_{ZZ} \gtrsim 600 \text{ GeV}$ . This high-mass distribution is displayed in Fig. 12, bottom left panel. There is also displayed the expected Standard Model background mainly due to processes  $gg, q\bar{q} \rightarrow ZZ$ . Observing that the expected Standard Model background is driven by sea partons, the  $ZZ$  invariant mass distribution should be exponentially suppressed in the high-mass region  $m_{ZZ} \gtrsim 500 \text{ GeV}$ . Indeed, this is clearly reproduced by numerical Monte Carlo simulations (see the red continuous lines in Fig. 12). From Fig. 12, bottom left panel, it should be evident that the number of events above  $m_{ZZ} \gtrsim 600 \text{ GeV}$  far exceeds the expected background. In addition, the events seem to be more densely distributed in the region around 700 GeV. This could signal the presence of a resonance with width  $\Gamma$  much more higher than the bin size 4 GeV. To enlighten this we have binned the events with a bin size of 20 GeV. The result, displayed in Fig. 12, bottom right panel, does indeed support the evidence of a broad structure around 700 GeV. In Fig. 12 we also compare the theoretical invariant-mass distribution of the heavy H Higgs boson to the experimental data. At this point it is necessary to precise that in our theoretical proposal, once the masses of the light Higgs boson  $h$  and the heavy Higgs boson  $H$  are fixed,  $m_h \simeq 125 \text{ GeV}$  and  $m_H \simeq 730 \text{ GeV}$ , there are no free parameters left to be tuned to better match the experimental observations. So that, the invariant-mass distribution in Fig. 12, bottom right panel, must be considered a prediction of our theory. Actually, we see that the theoretical distribution compares rather well with observations. Nevertheless, as a further check, we must wait for the release of the complete Run 2 dataset in the golden channel where the integrated luminosity should had increased by about a factor of two. Looking at Figs. 10 and 12 one could be led to the claim that the CMS Collaboration had found evidences for a new heavy resonance with central mass at 730 GeV and a rather large width. However, we do not have at our disposal the relevant LHC Run 2 datasets. Therefore, our phenomenological analysis, at best, should be considered as an indication of the presence of a new heavy resonance. Actually, the CMS Collaboration can easily perform full-fledged statistical analyses that can confirm or reject our theoretical proposal. On the other hand, it should be stressed that the results from the ATLAS Collaboration are not confirming the presence of a new heavy Higgs-like resonance. We already suggested that the effects of the tight selection cuts applied by the ATLAS Collaboration on the full Run 2 data could drastically reduce that sensitivity in the search of a broad heavy scalar resonance in the mass range 500 GeV - 1000 GeV. As a consequence we must wait for more data to settle the question.

We would like to conclude the present Section by emphasising that our heavy H resonance resembles a Standard Model Higgs boson since the inclusive production mechanisms are mainly by vector-boson fusion and gluon-gluon fusion processes. In addition, the main

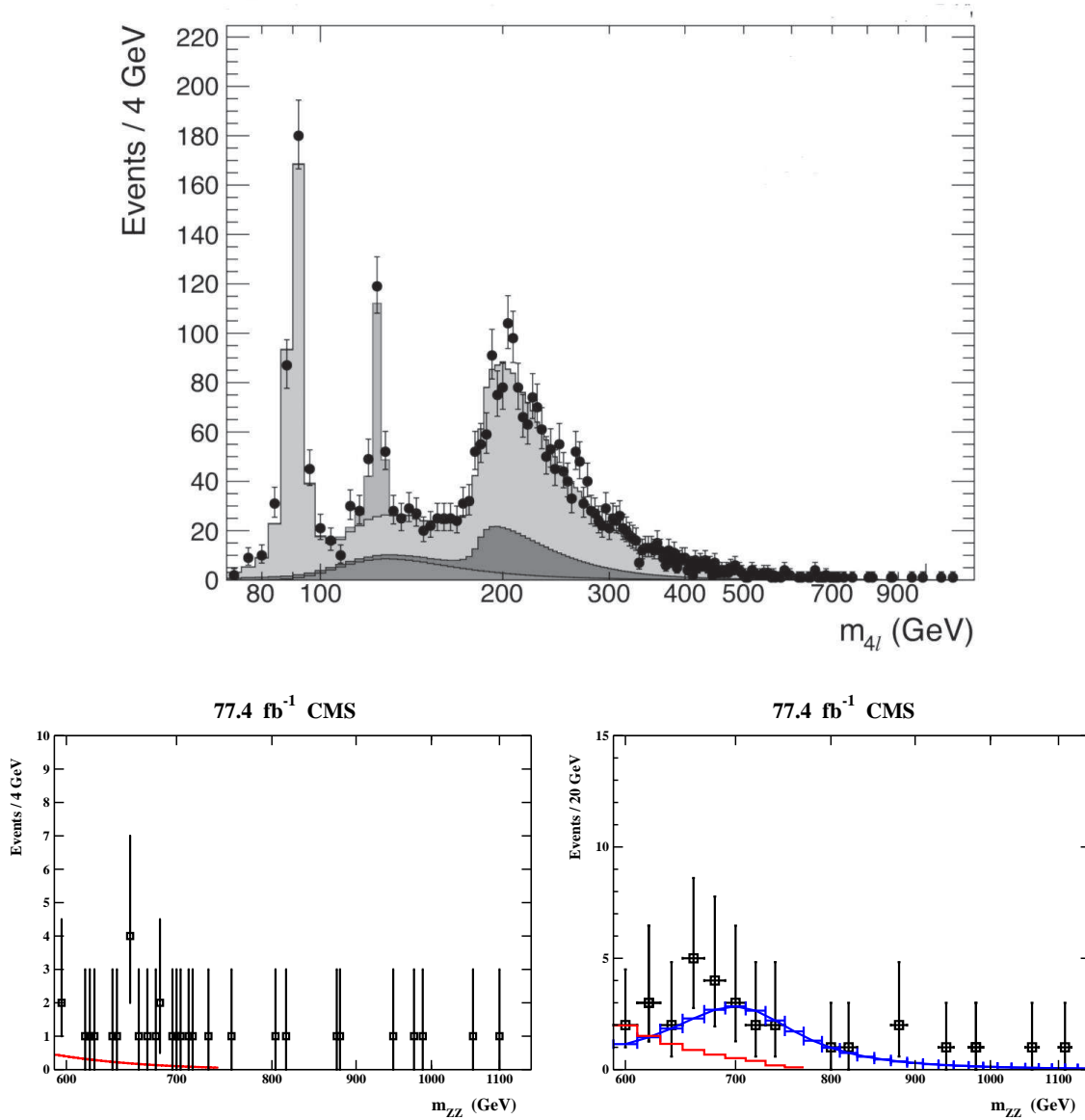


Figure 12: (Color online) (Upper panel) Distribution of the four-lepton reconstructed invariant mass  $m_{4\ell}$  in the full mass range combining the 2016 and 2017 CMS data. Adapted from Fig. 9 of Ref. [59]. Distribution of the invariant mass  $m_{ZZ}$ , with bin size 4 GeV (bottom left panel) and 20 GeV (bottom right panel) for the process  $H \rightarrow ZZ \rightarrow \ell\ell\ell\ell$  ( $\ell = e, \mu$ ) in the high-mass region  $m_{ZZ} \gtrsim 600$  GeV. Adapted from Fig. 1, left panels, of Ref. [46]. The (red) lines are the expected Standard Model background. The (blue) line is the expected signal histogram for our heavy Higgs boson.

decay modes are the decays  $H \rightarrow WW, ZZ$  with branching ratios satisfying Eq. (5.12).

## 6 Summary and conclusions

The Standard Model of the Elementary Particle Physics has been confirmed to a high level of precision by the experimental outcomes from the Large Hadron Collider. In particular, the discovery of a new narrow scalar resonance with mass 125 GeV, that resembles closely the Higgs boson, had firmly confirmed the Higgs mechanism, namely the spontaneous symmetry breaking of the electroweak gauge group by scalar fields. Nevertheless, from the theoretical point of view the widely accepted implementation of the Higgs mechanism is highly unsatisfying. In the perturbative approach to the spontaneous symmetry breaking of the gauge group one needs scalar fields with tachyonic mass term and positive quartic self-coupling. We repeatedly stressed that, from one hand there are no known physical mechanisms able to generate a negative mass squared for quantum scalar fields, on the other hand the triviality of self-interacting scalar quantum field theories invalidates the semi-classical perturbative implementation of the symmetry breaking. The unique way out left would be to consider the quantum scalar fields non-elementary or compound. Nevertheless, the absence of experimental evidences for physics beyond the Standard Model led us to esclude these possibilities.

In the first part of the paper we have illustrated the triviality and spontaneous symmetry breaking picture for the simplest scalar quantum field theory, namely the one-component scalar field. We showed that in that approach the spontaneous symmetry breaking could be driven by non-Gaussian quantum fluctuation despite the absence of a positive quartic self-coupling. However, we also found that that triviality and spontaneous symmetry breaking scenario cannot be realised within the pure scalar sector of the Standard Model. After that, we have carefully compared the perturbative and triviality and spontaneous symmetry breaking approaches to precise and extensive numerical results in the broken phase from the non-perturbative approach offered by the lattice formulation of the one-component scalar quantum field theory. We have shown that the proposal of triviality and spontaneous symmetry breaking compared rather well with numerical simulations, while the renormalised perturbative approach displayed statistically significant deviations with respect to the numerical results.

In the second part of the paper we addressed the problem of the spontaneous symmetry breaking in the Standard Model. As it is well known, in the Standard Model the presence of local gauge symmetries implies that to have the spontaneous symmetry breaking one is forced to fix the gauge. After that, in the unitary gauge the dynamics of the Standard Model scalar sector reduces to the one of the one-component scalar quantum field. Moreover, we found that the couplings of the scalar fields to the gauge vector bosons and fermions induce the needed non-Gaussian quantum fluctuations that, in turns, lead to the Bose-Einstein condensation. As a consequence, we obtained a clear physical picture of the Higgs mechanisms that is not subjected to the stability problem that affects the quantum vacuum in the perturbative approach. Moreover, we argued the the scalar Higgs condensate behave like a relativistic quantum liquid leading to the prevision of two Higgs bosons. The light Higgs boson resembles closely the new LHC narrow resonance at 125 GeV, while the heavy Higgs boson turns out to be a rather broad resonance with central mass of about 730 GeV. After discussing the phenomenological signatures of the heavy

Higgs boson, we looked at eventual experimental evidences by critically comparing our proposal to the complete LHC Run 2 data collected by the ATLAS and CMS Collaborations. We did not find convincingly evidences of the heavy Higgs boson in the ATLAS data. The CMS data, on the contrary, displayed evidences of a heavy Higgs boson in the main decay channels  $H \rightarrow WW, ZZ$  with reasonable statistical significance that compared favourably to our theoretical proposal. We, also, suggested that the discrepancies between the two experiments could originate from the severe selection cuts applied by the ATLAS Collaboration in they search of a heavy scalar resonance resembling a heavy Higgs boson.

In conclusions, the results presented in the present paper should have laid a solid theoretical basis for the eventual presence of an additional heavy Higgs boson. Of course, our theoretical proposal must wait for further LHC data to be validated. Nevertheless, we hope that our results will induce the LHC ATLAS and CMS Collaborations to undertake carefully searches of an eventual additional massive Higgs boson.

## References

- [1] F. Englert and R. Brout, Broken Symmetry and the Mass of Gauge Vector Mesons, Phys. Rev. Lett. **13** (1964) 321
- [2] P. Higgs, Broken symmetries, massless particles and gauge fields, Phys. Lett. **12** (1964) 132
- [3] G. Guralnik, C. Hagen and T. Kibble, Global Conservation Laws and Massless Particles, Phys. Rev. Lett. **13** (1964) 585
- [4] P. Higgs, Spontaneous Symmetry Breakdown without Massless Bosons, Phys. Rev. **145** (1966) 1156
- [5] The ATLAS Collaboration, G. Aad, *et al.*, Observation of a new particle in the search for the Standard Model Higgs boson with the ATLAS detector at the LHC, Phys. Lett. B **716** (2012) 1
- [6] The CMS Collaboration, S. Chatrchyan, *et al.*, Observation of a New Boson at a Mass of 125 GeV with the CMS Experiment at the LHC, Phys. Lett. B **716** (2012) 30
- [7] R. Fernandez, J. Fröhlich, and A. D. Sokal, RandomWalks, Critical Phenomena, and Triviality in Quantum Field Theory, Springer, Berlin, Germany, 1992.
- [8] M. Aizenman and H. Duminil-Copin, Marginal triviality of the scaling limits of critical 4D Ising and  $\phi_4^4$  models, Ann. Math. **194** (2021) 163
- [9] R. F. Streater and A. S. Weightman, PCT, Spin and Statistic, and all that, W. A. Benjamin, INC., New York, Amsterdam, 1964
- [10] F. Strocchi, General Properties of Quantum Field Theory, World Scientific Publishing Co. Ptc. Ltd., Singapore, New Jersey, London, Hong Kong, 1993

- [11] A. S. Weightman, La theorie quantique locale et la theorie quantique des champs, *Ann. Inst. H. Poincare* **I** (1964) 403
- [12] R. Haag, On Quantum Field Theories, *Danske Videnskabernes Selskab Matematisk-Fysiske Meddelelser* **29** (1955) 1
- [13] J. Earman and D. Fraser, Haag’s Theorem and its Implications for the Foundations of Quantum Field Theory, *Erkenntnis* **64** (2006) 305
- [14] L. Klaczynski, Haag’s Theorem in renormalised Quantum Field Theories, *arXiv:1602.00662* (2016)
- [15] A. Duncan, *The Conceptual Framework of Quantum Field Theory*, Oxford University Press, Great Clarendon Street, Oxford, United Kingdom, 2012
- [16] F. Strocchi, *An Introduction to Non-Perturbative Foundations of Quantum Field Theory*, Oxford University Press, Oxford, United Kingdom, 2013
- [17] K. Symanzik, Schrödinger representation and Casimir effect in renormalizable quantum field theory, *Nucl. Phys.* **B 190** [FS3] (1981) 1
- [18] S. Coleman and E. J. Weinberg, Radiative Corrections as the Origin of Spontaneous Symmetry Breaking, *Phys. Rev. D* **7** (1973) 1888
- [19] E. J. Weinberg, Radiative Corrections as the Origin of Spontaneous Symmetry Breaking, Ph.D. thesis, 1973, *arXiv:hep-th/0507214* (2005)
- [20] M. Consoli and P. M. Stevenson, The non-trivial effective potential of the ‘trivial’  $\lambda\Phi^4$  theory: A lattice test, *Z. Phys. C* **63** (1994) 427
- [21] M. Consoli and P. M. Stevenson, Mode-dependent field renormalization and triviality in  $\lambda\Phi^4$  theory, *Phys. Lett.* **B 391** (1994) 144
- [22] P. Cea, The Higgs Condensate as a Quantum Liquid, *International Journal of Theoretical Physics* **59** (2020) 3310
- [23] N. N. Bogolubov, On the theory of superfluidity, *J. Phys. (USSR)* **11** (1947) 23
- [24] K. Osterwalder and R. Schrader, Axioms for Euclidean Green’s functions, *Commun. Math. Phys.* **31** (1973) 83
- [25] K. Osterwalder and R. Schrader, Axioms for Euclidean Green’s functions II, *Commun. Math. Phys.* **42** (1975) 281
- [26] C. B. Lang, Computer Stochastics in Scalar Quantum Field Theory, in *Stochastic Analysis and Applications in Physics*, NATO ASI Series 449, Edited by: A. I. Cardoso, M. de Faria, J. Potthoff, R. Sénéor, L. Streit, Springer Science+Business Media Dordrecht, 1994
- [27] M. Lüscher and P. Weisz, Scaling laws and triviality bounds in the lattice  $\phi^4$  theory. 1. One-component model in the symmetric phase, *Nucl. Phys.* **B 290** (1987) 25



- [28] M. Lüscher and P. Weisz, Scaling laws and triviality bounds in the lattice  $\phi^4$  theory. 2. One-component model in the phase with spontaneous symmetry breaking, Nucl. Phys. **B 295** (1988) 65
- [29] A. Agodi, G. Andronico, P. Cea, M. Consoli, L. Cosmai, R. Fiore and P. M. Stevenson, A Lattice test of alternative interpretations of "triviality" in  $(\lambda\Phi^4)_4$  theory, Mod. Phys. Lett. A **12** (1997) 1011
- [30] A. Agodi, G. Andronico, P. Cea, M. Consoli and L. Cosmai, The  $(\lambda\Phi^4)_4$  theory on the lattice: effective potential and triviality, Nucl. Phys. B (Proc. Suppl.) **63A-C** (1998) 637
- [31] D. S. Gaunt, M. F. Sykes, and S. McKenzie, Susceptibility and fourth-field derivative of the spin  $\frac{1}{2}$  Ising model for  $T > T_c$  and  $d = 4$ , J. Phys. **A12** (1979) 871
- [32] P. Cea, M. Consoli, and L. Cosmai (2005), Large logarithmic rescaling of the scalar condensate: new lattice evidences, hep-lat/0501013 (2005)
- [33] P. Cea and L. Cosmai, The Higgs boson: From the lattice to LHC, ISRN High Energy Physics, vol. 2012, Article ID 637950, arXiv:0911.5220 (2012).
- [34] R. H. Swendsen and J.-S. Wang, Nonuniversal critical dynamics in Monte Carlo simulations, Phys. Rev. Lett. **58** (1987) 86
- [35] U. Wolff, Collective Monte Carlo updating for spin systems, Phys. Rev. Lett. **62** (1989) 361
- [36] J. Balog, A. Duncan, R. Willey, F. Niedermayer, and P. Weisz, The 4d one component lattice  $\phi^4$  model in the broken phase revisited, Nucl. Phys. **B 714** [FS] (2005) 256
- [37] P. M. Stevenson, Comparison of perturbative RG theory with lattice data for the 4d Ising model, Nucl. Phys. **B 729** (2005) 542
- [38] J. Balog, F. Niedermayer and P. Weisz, Repairing Stevenson's step in the 4d Ising model, Nucl. Phys. **B 741** (2006) 390
- [39] E. Brezin, J. C. Guillou and J. Zinn-Justin, Field Theoretical Approach to Critical Phenomena, in Phase transitions and Critical Phenomena, Vol. 6, edited by C. Domb and M. S. Green, Academic Press Inc., London, 1976
- [40] J. Zinn-Justin, Quantum Field Theory and Critical Phenomena, Fourth Edition, Clarendon Press, Oxford, 2002
- [41] K. Kenna and C. B. Lang, Renormalization group analysis of finite-size scaling in  $\phi_4^4$  model, Nucl. Phys. **B 393** (1993) 461
- [42] K. Kenna and C. B. Lang, Scaling and density of Lee-Yang zeros in the four-dimensional Ising model, Phys. Rev. E **49** (1994) 5012
- [43] Pik-Yin Lai and K. K. Mon, From Finite-size scaling of the Ising model in four dimensions, Phys. Rev. B **41** (1990) 9257

- [44] M. Lüscher and P. Weisz, Scaling laws and triviality bounds in the lattice  $\phi^4$  theory (III). n-component model, Nucl. Phys. **B 318** (1989) 705
- [45] S. Elitzur, Impossibility of Spontaneously Breaking Local Symmetries, Phys. Rev. **D 12** (1975) 3978
- [46] P. Cea, Evidence of the true Higgs boson  $H_T$  at the LHC Run 2, Mod. Phys. Lett. **A 34** (2019) 1950137
- [47] BSM Higgs production cross sections at  $\sqrt{s}=13$  TeV (update in CERN Report4 2016) [/twiki.cern.ch/twiki/bin/view/LHCPhysics/CERNYellowReportPageBSMAt13TeV](https://twiki.cern.ch/twiki/bin/view/LHCPhysics/CERNYellowReportPageBSMAt13TeV)
- [48] J. F. Gunion, H. E. Haber, G. Kane, and S. Dawson, The Higgs Hunter's Guide, Perseus Publishing, Cambridge, Massachusetts, 1990
- [49] A. Djouadi, The Anatomy of Electro-Weak Symmetry Breaking. I: The Higgs boson in the Standard Model, Phys. Rept. **457** (2008) 1
- [50] G. Breit and E. P. Wigner, Capture of Slow Neutrons, Phys. Rev. **49** (1936) 519
- [51] P. Cea, The Higgs condensate as a quantum liquid: Comparison with the ATLAS full Run 2 data, arXiv:2111.10833 [hep-ph] (2021)
- [52] M. Aaboud *et al.*, the ATLAS Collaboration, Search for heavy  $ZZ$  resonances in the  $\ell^+\ell^-\ell^+\ell^-$  and  $\ell^+\ell^-\nu\bar{\nu}$  final states using proton-proton collisions at  $\sqrt{s} = 13$  TeV with the ATLAS detector, Eur. Phys. J. C **78** (2018) 293
- [53] G. Aad *et al.*, the ATLAS Collaboration, Search for heavy resonances decaying into a pair of Z bosons in the  $\ell^+\ell^-\ell^+\ell^-$  and  $\ell^+\ell^-\nu\bar{\nu}$  final states using 139 fb $^{-1}$  of proton-proton collisions at  $\sqrt{s} = 13$  TeV with the ATLAS detector, Eur. Phys. J. C **81** (2021) 332
- [54] G. Aad *et al.*, the ATLAS Collaboration, Search for heavy diboson resonances in semileptonic final states in  $pp$  collisions at  $\sqrt{s} = 13$  TeV with the ATLAS detector, Eur. Phys. J. C **80** (2020) 1165
- [55] The ATLAS Collaboration, Search for heavy resonances in the decay channel  $W^+W^- \rightarrow e\nu\mu\nu$  in  $pp$  collisions at  $\sqrt{s} = 13$  TeV using 139 fb $^{-1}$  of data with the ATLAS detector, ATLAS-CONF-2022-066 (2022)
- [56] The CMS Collaboration, Search for high mass resonances decaying into  $W^+W^-$  in the dileptonic final state with 138 fb $^{-1}$  of proton-proton collisions at  $\sqrt{s} = 13$  TeV, CMS PAS HIG-20-016 (2022)
- [57] P. Cea, The Higgs condensate as a quantum liquid: Comparison with the full Run 2 CMS data, arXiv:2205.12234 [hep-ph] (2022)
- [58] E. Gross and O. Vitells, Trial factors for the look elsewhere effect in high energy physics, Eur. Phys. J. C **70** (2010) 525
- [59] The CMS Collaboration, Measurements of properties of the Higgs boson in the four-lepton final state at  $\sqrt{s} = 13$  TeV, CMS PAS HIG-18-001 (2018)